

Material and methods

Patients, tumor specimens and cell lines

One hundred and eight tumor specimens used in the present study were kindly provided from various institutions and hospitals in Japan (see Supplementary Information). Informed consent was obtained at each institution or hospital. All tumors were diagnosed clinically as well as pathologically as neuroblastoma and staged according to the International Neuroblastoma Staging System (INSS) criteria.¹⁷ Twenty-seven patients were Stage 1, 15 Stage 2, 36 Stage 3, 23 Stage 4 and 7 Stage 4S. The patients were treated by the standard protocols as described previously.^{18,19} *MYCN* copy number, *TrkA* mRNA expression levels and DNA index were measured as reported previously.²⁰ Our present study was approved by the Institutional Review Board of the Chiba Cancer Center (CCC7817).

Human tumor-derived cell lines were cultured in RPMI 1640 medium (Nissui, Tokyo, Japan) supplemented with 10% heat-inactivated fetal bovine serum (FBS, Invitrogen, Carlsbad, CA) and 50 µg/ml penicillin/streptomycin (Invitrogen) in an incubator with humidified air at 37°C with 5% CO₂.

Array-comparative genomic hybridization

Array-CGH analysis was performed using UCSF BAC array (2464 BACs, ≈1 Mb resolution) with 236 primary neuroblastomas. Detailed experimental procedures and the criteria for losses and gains were described previously.^{3,20-22}

LOH analysis

Genomic DNA prepared from neuroblastomas and bloods was amplified by PCR-based strategy using the primer set, one of which was labeled with fluorescent dye CY5. The amplified fragments including 3 polymorphic STS markers encompassing *TSLC1*, *D11S4111*, *D11S2077* and *D11S1885*, were separated by 6% polyacrylamide gels containing 6 M urea using an automated ALF express DNA sequencer.

Semiquantitative and quantitative reverse transcription-PCR analysis

Total RNA was prepared from the indicated primary neuroblastomas, various human normal tissues and tumor-derived cell lines were subjected to semiquantitative RT-PCR using SuperScript II reverse transcriptase and random primers (Invitrogen), according to the manufacturer's instructions. Oligonucleotide primer set used to amplify *TSLC1* by semiquantitative RT-PCR was as follows: 5'-CATTITGGAAATTTGCCTGCT-3' (sense) and 5'-GGCAGCAGCAAAGAG TTTTC-3' (antisense). Quantitative real-time PCR was carried out using TaqMan(R) Gene Expression Assay System (Applied Biosystems, Foster City, CA) as described previously.²⁰ In brief, expression levels were calculated as a ratio of mRNA level for a given gene relative to mRNA for *GAPDH* in the same cDNA. The oligonucleotide primers and TaqMan probes, labeled at the 5'-end with the reporter dye 6-carboxyfluorescein (FAM) and at the 3'-end with 6-carboxyteramethylrhodamine (TAMRA), were provided by Applied Biosystems (Hs00942508_m1).

Immunohistochemistry

A 4-µm-thick section of formalin-fixed, paraffin-embedded tissues were stained with hematoxylin and eosin and the adjacent sections were immunostained for *TSLC1* using polyclonal anti-*TSLC1* antibody (CC2) as described previously.¹⁰ The BenchMark XT immunostainer (Ventana Medical Systems, Tucson, AZ) and 3-3' diaminobenzidine detection kit (Ventana Medical Systems) were used to visualize *TSLC1*. Appropriate positive and negative control experiments were also performed in parallel for each immunostaining.

Small interfering RNA

TSLC1 siRNA (GUCAAUAAGAGUGACGACUUU) and Stealth RNAi Negative Control Duplex were purchased from Sigma-Aldrich (St. Louis, MO) and Invitrogen, respectively.

Transfection

Neuroblastoma-derived SH-SY5Y cells were transfected with the indicated combinations of expression plasmids or with siRNA against *TSLC1* using LipofectAMINE 2000 or LipofectAMINE RNAiMAX transfection reagent (Invitrogen), according to the manufacturer's recommendations.

Colony formation assay

SH-SY5Y and SK-N-AS cells (1×10^5 cells/plate) were seeded in 6-well cell culture plates and transfected with or without the increasing amounts of the expression plasmid for *TSLC1* (0, 250, 750 or 1,000 ng). Total amounts of plasmid DNA per transfection were kept constant (1 µg) with the empty plasmid (pcDNA3.1-Hygro (+); Invitrogen). Forty-eight hours after transfection, cells were transferred into the fresh medium containing hygromycin (at a final concentration of 200 µg/ml) and maintained for 14 days. Drug-resistant colonies were then stained with Giemsa's solution and numbers of drug-resistant colonies were scored.

Cell growth assay

SH-SY5Y cells (6×10^5 cells/dish) were seeded in 10-cm diameter cell culture dish and transiently transfected with siRNA against *TSLC1* (240 pmol). Thirty-six hours after transfection, 2×10^4 cells were transferred into 6-well plates and transfected with 60 pmol of siRNA against *TSLC1*. At the indicated time points after transfection, number of viable cells was measured using a Coulter Counter (Coulter Electronics, Hialeah, Finland).

Bisulfite-sequencing

Sodium bisulfite-mediated modification of genomic DNA was performed using Bisulfite Methylated DNA Detection Kit (Toyobo, Osaka, Japan), according to the manufacturer's instructions. Modified genomic DNA was subjected to PCR-based amplification with a primer set as described previously.²³ The PCR products containing the promoter region of *TSLC1* gene were purified by PCR Purification Kit (Qiagen, Valencia, CA) and their nucleotide sequences were determined by using a 3730 DNA Analyzer (Applied Biosystem).

Statistical analysis

Fisher's exact tests were employed to examine possible associations between *TSLC1* expression and other prognostic indicators such as age. The difference between high and low expression levels of *TSLC1* was based on the mean value obtained from quantitative real-time PCR analysis. Kaplan-Meier survival curves were calculated, and survival distributions were compared using the log-rank test. Cox regression models were used to investigate the associations between *TSLC1* expression levels, age, *MYCN* amplification status, INSS and survival. Differences were considered significant if the *p*-value was less than 0.05.

Results

Array-comparative genomic hybridization analysis identifies the smallest region of overlaps of deletion in neuroblastoma at 11q23

We have previously performed array-CGH analysis using UCSF BAC array (2464 BACs, ≈1-Mb resolution) and 236 primary neuroblastomas.³ In our array-CGH study, 66 tumors were revealed to have partial deletion of 11q as shown in Figure 1a, whose SRO were approximately 10-Mb long at 11q23 (from physical location of 110,979 to 119,806 kb in UCSC database, May 2006). To date, the data base analysis demonstrated that there could exist approximately 100 genes within this region. Of inter-

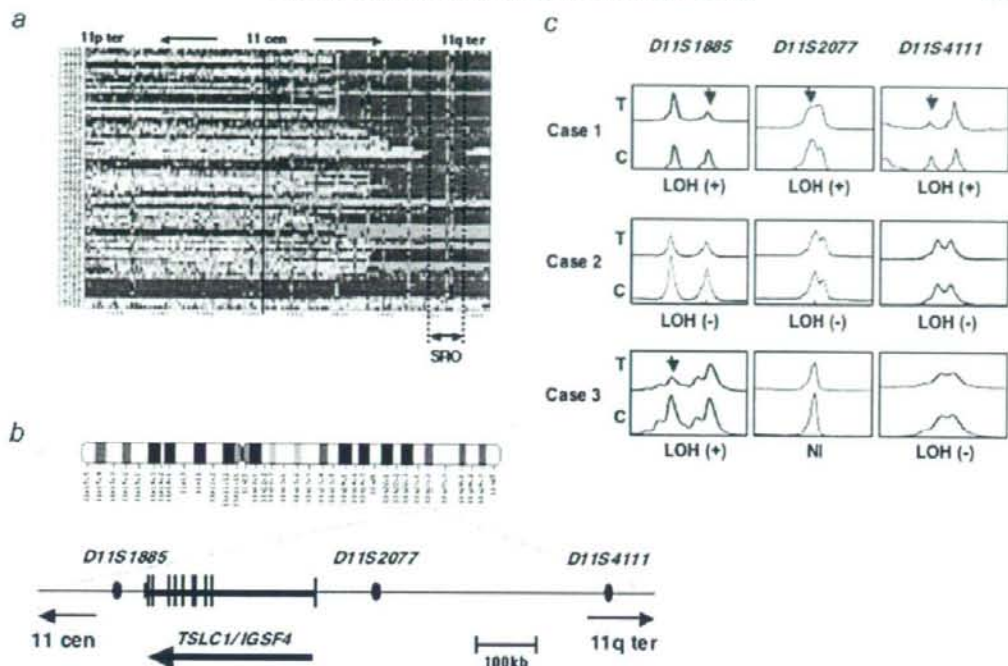


FIGURE 1 – Identification of the SRO of deletion at 11q in primary neuroblastoma. (a) Array-CGH analysis. Blue color indicates the position of the deleted area in each case. The smallest region of overlaps (SRO) of deletion at 11q is also shown. (b) The schematic drawing of the relative positions of 3 independent polymorphic markers at 11q23 used in the present study and *TSLC1* gene on human chromosome 11. (c) Representative electropherograms obtained from LOH analysis. Genomic DNA prepared from primary tumors (T) and their corresponding blood (C) was subjected to LOH analysis. Allelic losses are indicated by arrowheads. NI, not informative.

est, *TSLC1* gene which has been considered as a putative tumor suppressor for human lung as well as other cancers⁹ locates within this region (Fig. 1b). These observations prompted us to perform loss of heterozygosity (LOH) as well as expression studies of *TSLC1* gene in primary neuroblastoma.

LOH at the TSLC1 locus is frequently detected in primary neuroblastoma

According to the previous observations,^{9,24} tumor-specific downregulation of *TSLC1* gene might be largely attributed to loss of one allele in association with the hypermethylation of its promoter region in the remaining allele. To address whether LOH of *TSLC1* locus could be frequently detectable in primary neuroblastoma, we carried out LOH analysis using 3 independent fluorescently labeled polymorphic microsatellite markers (*D11S1885*, *D11S2077* and *D11S4111*) surrounding *TSLC1* gene (Fig. 1b). In accordance with the previous results,^{9,25,26} the incidence of 11q23 LOH was 22% (7 of 32) and 45% (18 of 40) in favorable neuroblastomas (Stage 1 or 2) and unfavorable ones (Stage 3 or 4), respectively (data not shown). Statistical Fisher's exact test analysis revealed that the presence of LOH at this locus is associated with unfavorable neuroblastomas ($p = 0.0493$; data not shown). It is worth noting that LOH is detectable at *D11S1885* but not at *D11S4111* in Case 3 tumor (Fig. 1c), indicating that a putative chromosome breakpoint might exist between these loci.

Downregulation of TSLC1 expression is frequently observed in unfavorable neuroblastomas

Based on the previous observations,¹¹⁻¹⁶ the expression levels of *TSLC1* were significantly reduced in advanced stages of tumors as compared with those in early stages of tumors. We then examined the expression levels of *TSLC1* in 16 favorable neuroblastomas without *MYCN* amplification and 16 unfavorable ones with *MYCN* amplification. As clearly shown in Figure 2a, *TSLC1* was expressed at lower levels in unfavorable neuroblastomas relative to favorable ones as examined by semiquantitative RT-PCR. To ask whether there could exist a possible relationship between downregulation of *TSLC1* and *MYCN* amplification, we examined the expression levels of *TSLC1* in various neuroblastoma-derived cell lines bearing single copy of *MYCN* or *MYCN* amplification. As shown in Supplementary Figure 1a, a significant downregulation of *TSLC1* expression was detected in 2 of 6 neuroblastoma cell lines carrying single copy of *MYCN* (OAN and CNB-RT) and in 4 of 21 (CHP134, KP-N-NS, SK-N-DZ and NMB) bearing *MYCN* amplification as examined by semiquantitative RT-PCR. In addition, there was no obvious correlation between the expression levels of *TSLC1* and loss of 11q except OAN, SK-N-DZ and NMB. Next, we checked the expression levels of *TSLC1* in various human adult and fetal tissues. As seen in Supplementary Figure 1b, *TSLC1* was highly expressed in normal neuronal tissues, adrenal gland, testis, prostate and liver. Our present results suggest that *TSLC1* is expressed in normal neuronal tissues and its expression levels might be regulated in a *MYCN*-dependent manner in

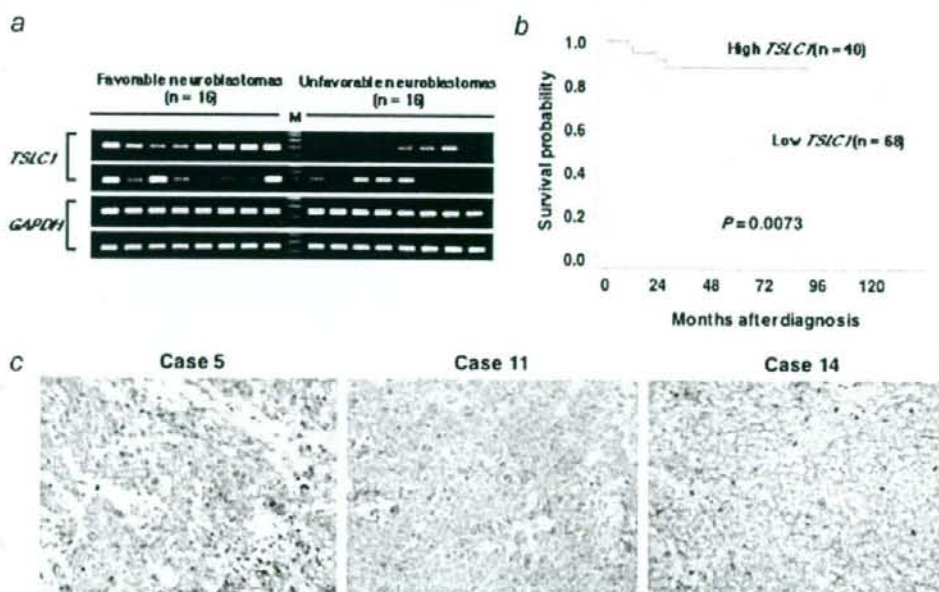


FIGURE 2 – Expression levels of *TSLC1* in primary neuroblastomas. (a) Expression of *TSLC1* in 16 favorable neuroblastomas bearing single copy of *MYCN* (Stage 1, higher expression levels of *TrkA*) and 16 unfavorable ones carrying *MYCN* amplification (stages 3 and 4, lower expression levels of *TrkA*). Total RNA was prepared from the indicated neuroblastoma tissues, reverse transcribed and amplified by PCR to examine the expression levels of *TSLC1*. *GAPDH* serves as an internal control. (b) Kaplan-Meier survival curves of patients with neuroblastomas based on higher or lower expression levels of *TSLC1*. Expression levels of *TSLC1* in 108 primary neuroblastoma samples categorized by their clinical stage were examined by a quantitative real-time PCR. Relative expression levels of *TSLC1* mRNA were determined by calculating the ratio between *GAPDH* and *TSLC1*. (c) Immunohistochemical analysis. Tumor samples derived from Case 5 (favorable neuroblastoma bearing single copy of *MYCN*), Case 11 (unfavorable neuroblastoma with *MYCN* amplification) and Case 14 (unfavorable neuroblastoma carrying single copy of *MYCN*) were fixed and stained with polyclonal anti-*TSLC1* antibody.

primary neuroblastoma but not in neuroblastoma-derived cell lines.

Lower expression levels of *TSLC1* are associated with poor outcome of neuroblastoma

To evaluate whether there could exist a possible relationship between *TSLC1* expression levels and clinicopathological factors of neuroblastoma patients, we have performed a quantitative real-time PCR. For this purpose, total RNA prepared from 108 primary neuroblastoma samples was subjected to a quantitative real-time PCR. According to the mean values of its expression levels obtained from a quantitative real-time PCR, these patients were divided into 2 groups including 40 patients with tumors expressing higher levels of *TSLC1* (High *TSLC1*) and 68 patients with tumors expressing lower levels of *TSLC1* (Low *TSLC1*). As shown in Table I, the significant differences were detectable between the above-mentioned 2 groups with respect to INSS stage, Shimada's pathological classification, copy number of *MYCN*, *TrkA* expression levels and DNA index. In contrast, no significant differences were observed between them with respect to their age, tumor origin and LOH on *TSLC1* locus.

We then examined whether there could exist a possible correlation between the expression levels of *TSLC1* in primary neuroblastomas and the survival of patients with neuroblastomas. The log-rank test showed that lower expression levels of *TSLC1* significantly correlate with unfavorable outcome ($p = 0.007$) as shown

TABLE I – CORRELATION BETWEEN *TSLC1* EXPRESSION AND OTHER PROGNOSTIC FACTORS OF NEUROBLASTOMA

| Terms | <i>TSLC1</i> expression | | p-Value |
|-------------------------|-------------------------------|------------------------------|---------|
| | High <i>TSLC1</i> (n = 40) | Low <i>TSLC1</i> (n = 68) | |
| Age (year) | | | |
| <1.5 | 23 | 29 | |
| >1.5 | 17 | 39 | 0.1646 |
| Tumor origin | | | |
| Adrenal gland | 20 | 36 | |
| Others | 20 | 30 | 0.6915 |
| Stage | | | |
| 1, 2, 4S | 24 | 25 | |
| 3, 4 | 16 | 43 | 0.0274 |
| Shimada pathology | | | |
| Favorable | 31 | 35 | |
| Unfavorable | 6 | 22 | 0.0227 |
| <i>MYCN</i> copy number | | | |
| Single | 38 | 51 | |
| Amplified | 2 | 17 | 0.0086 |
| <i>TrkA</i> expression | | | |
| High | 28 | 28 | |
| Low | 12 | 37 | 0.0090 |
| DNA index | | | |
| Diploidy | 8 | 39 | |
| Aneuploidy | 28 | 19 | <0.0001 |
| LOH | | | |
| (-) | 18 | 29 | |
| (+) | 9 | 16 | >0.9999 |

TABLE II - IMMUNOHISTOCHEMICAL ANALYSIS OF TSLC1 EXPRESSION IN PRIMARY NEUROBLASTOMAS

| Case | Age/Gender | MYCN | INPC | Primary site | Stage (INSS) | TSLC1 |
|------|------------|------|---------------------------------------|--------------|--------------|----------------------|
| 4 | 6 m/M | NA | NBL, Poorly diff., Low MKI, FH | Mediastinum | Stage 1 | (+) |
| 5 | 7 m/M | NA | NBL, Poorly diff., Low MKI, FH | Adrenal | Stage 1 | (+) |
| 6 | 9 m/M | NA | NBL, Poorly diff., Low MKI, FH | Adrenal | Stage 1 | (+) |
| 7 | 25 m/M | NA | NBL, Differentiating, Low MKI, FH | Adrenal | Stage 4 | (+) |
| 8 | 29 m/M | NA | NBL, Differentiating, Low MKI, FH | Mediastinum | Stage 2 | (+) |
| 9 | 13 m/M | A | NBL, Poorly diff., High MKI, UH | Adrenal | Stage 4 | (-) |
| 10 | 13 m/M | A | NBL, Poorly diff., Low MKI, UH | Abdominal | Stage 4 | (-) |
| 11 | 18 m/M | A | NBL, Poorly diff., Low MKI, UH | Adrenal | Stage 3 | (-) |
| 12 | 8 y/M | NA | NBL, Poorly diff., Low MKI, UH | Adrenal | Stage 4 | (+) |
| 13 | 8 m/M | NA | nGNB (NBL, poorly diff., Low MKI), UH | Mediastinum | Stage 2 | (-)/(+) ¹ |
| 14 | 20 m/M | NA | NBL, Poorly diff., Low MKI, UH | Adrenal | Stage 3 | (+) |

m, months; y, years; M, male; NA, not amplified; A, amplified; NBL, neuroblastoma; nGNB, nodular ganglioneuroblastoma; MKI, mitosis-karyorrhexis index; FH, favorable histology; UH, unfavorable histology; (+), positive; (-), negative.

¹Neuroblastoma component showed negative of TSLC1 signals, whereas ganglioneuroma showed positive of TSLC1 signals.

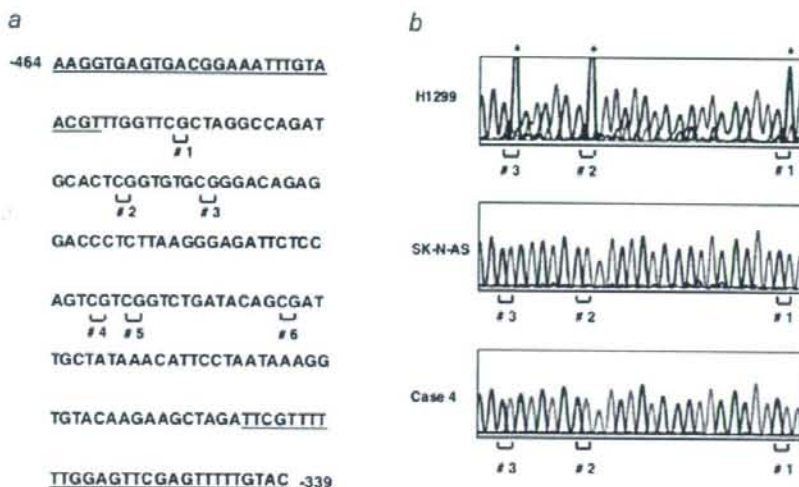


FIGURE 3 - Bisulfite-sequencing analysis of TSLC1 gene promoter in neuroblastoma-derived cell lines and primary neuroblastomas. (a) Nucleotide sequence spanning from -464 to -339 relative to the translational initiation site (+1). Six CpG sites are shown. Primer sequences used for PCR-based amplification are underlined. (b) Bisulfite-sequencing analysis. Sequencing histograms showing the methylation status of CpG sites (#1, #2 and #3) are depicted. Asterisks indicate the positions of the methylated cytosine residues at the indicated CpG sites. H1299 cells were used as a positive control. [Color figure can be viewed in the online issue, which is available at www.interscience.wiley.com.]

in Kaplan-Meier cumulative survival curves (Fig. 2b and Supplementary Table I). Additionally, multivariable Cox analysis demonstrated that only clinical stage and MYCN amplification are significantly associated with their survival (Supplementary Table II), suggesting that TSLC1 expression levels strongly correlate with these factors.

To further confirm the expression levels of TSLC1 in primary neuroblastomas, we employed immunohistochemical staining of TSLC1 in 11 primary neuroblastomas, including 5 favorable neuroblastomas bearing single copy of MYCN, 3 unfavorable neuroblastomas carrying single copy of MYCN and 3 unfavorable neuroblastomas with MYCN amplification. As shown in Figure 2c, TSLC1 appeared to be detectable at the cell-cell boundary of the tumors (cases 5 and 14) but not in Case 11. The immunohistochemical data were summarized in Table II. TSLC1 was detectable in tumors with favorable histology bearing single copy of MYCN (cases 4-8), whereas cases 9-11 with unfavorable histology carrying MYCN amplification did not express TSLC1. In addition, Case 13 was a nodular ganglioneuroblastoma whose ganglioneuroma and neuroblastoma components were TSLC1-positive and -negative, respectively. Of note, TSLC1 was detected in

tumors with unfavorable histology bearing single copy of MYCN (cases 12-14). These observations indicate that there exists an inverse relationship between the expression levels of TSLC1 and MYCN amplification in primary neuroblastomas.

No promoter methylation of TSLC1 gene in neuroblastoma cell lines and primary neuroblastomas

Based on our present results, lower expression levels of TSLC1 gene in unfavorable neuroblastomas might not be due to allelic loss of TSLC1 locus. Since accumulating evidence strongly suggests that the downregulation of TSLC1 in several cancers is associated with the hypermethylation of its promoter region,^{9,11,12,24,26-29} we sought to examine whether the hypermethylation of TSLC1 promoter region could be detectable in unfavorable neuroblastomas. For this purpose, we directly examined the methylation status of 6 cytosine residues of CpG sites within a putative TSLC1 promoter region (Fig. 3a) by bisulfite-sequencing in 27 cell lines and 115 primary neuroblastomas. Sodium bisulfite modification of genomic DNA converts unmethylated cytosine residues to uracil residues but does not affect methylated cytosine residues. Unexpectedly, methylated cytosines

were undetectable in all primary neuroblastomas and cell lines, whereas hypermethylation was readily detected in human lung adenocarcinoma-derived H1299 cell line used as a positive control (Fig. 3b). Our present findings ruled out the possibility that the hypermethylation of *TSLC1* promoter region contributes to the downregulation of *TSLC1* gene in unfavorable neuroblastomas. Of note, the treatment of neuroblastoma-derived SH-SY5Y and CHP-134 cells with TSA (trichostatin A) resulted in a remarkable upregulation of *TSLC1* (Fig. 4). Since TSA is a histone deacetylase in-

hibitor, it is possible that the acetylation status of histone plays an important role in the regulation of *TSLC1* expression.

TSLC1 has an ability to suppress cell growth of neuroblastoma cells

To examine whether *TSLC1* could have an ability to suppress neuroblastoma cell proliferation, we performed colony formation assays. Neuroblastoma-derived SH-SY5Y cells were transfected with or without the increasing amounts of the *TSLC1* expression plasmid and maintained in fresh medium containing hygromycin for 14 days. As shown in Figure 5a, number of drug-resistant colonies was significantly reduced in a dose-dependent manner as compared with that in cells transfected with the empty plasmid alone. Similar results were also obtained in neuroblastoma-derived SK-N-AS cells (Supplementary Fig. 2). Next, we sought to examine a possible effect of the endogenous *TSLC1* on neuroblastoma cell growth. To this end, SH-SY5Y cells were transiently transfected with control siRNA or siRNA against *TSLC1*. As shown in Figure 5b, siRNA-mediated silencing of the endogenous *TSLC1* was successful under our experimental conditions. Consistent with the present results obtained from colony formation assays, siRNA-mediated knockdown of *TSLC1* resulted in an accelerated cell proliferation relative to the control cells ($p < 0.05$). Thus, it is likely that *TSLC1* has an ability to suppress neuroblastoma cell proliferation.

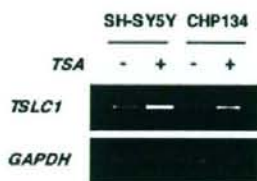


FIGURE 4 – Upregulation of *TSLC1* in cells exposed to TSA. SH-SY5Y and CHP-134 cells were treated with TSA (at a final concentration of 100 ng/ml) or left untreated. Twelve hours after treatment, total RNA was prepared and analyzed for the expression levels of *TSLC1* by semiquantitative RT-PCR. *GAPDH* was used as an internal control.

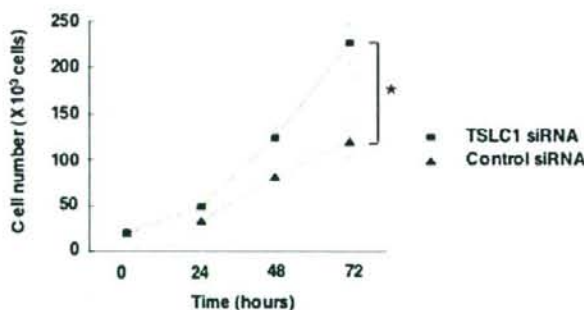
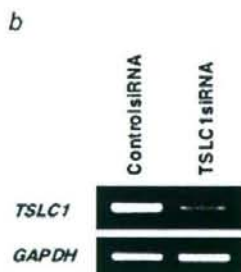
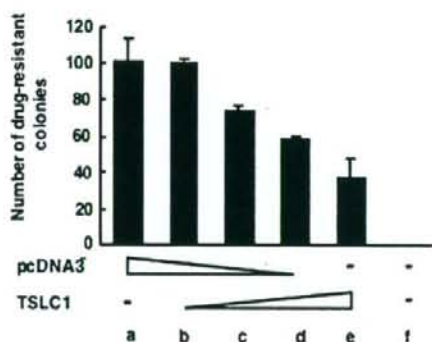
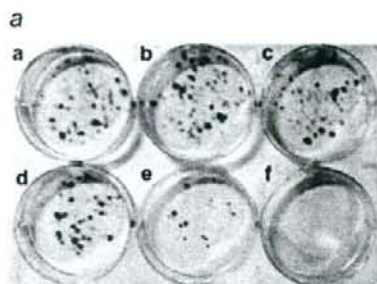


FIGURE 5 – Growth-suppressive potential of *TSLC1* in neuroblastoma cells. (a) Colony formation assay. SH-SY5Y cells were transfected with the increasing amounts of the expression plasmid for *TSLC1* (0, 250, 750 or 1,000 ng). Total amounts of plasmid DNA per transfection were kept constant (1 μ g) with pcDNA3. Forty-eight hours after transfection, cells were transferred into the fresh medium containing hygromycin (at a final concentration of 200 μ g/ml) and incubated for 2 weeks. Drug-resistant colonies were stained with Giemsa's solution (left panel) and number of drug-resistant colonies was scored (right panel). (b) siRNA-mediated knockdown of *TSLC1*. SH-SY5Y cells were transiently transfected with control siRNA or with siRNA against *TSLC1*. Forty-eight hours after transfection, total RNA was prepared and subjected to semiquantitative RT-PCR (left panel). At the indicated time periods after transfection, number of viable cells was measured in triplicate (right panel). The differences between the growth rate of control cells and *TSLC1*-knocked down cells were statistically significant ($p < 0.05$). [Color figure can be viewed in the online issue, which is available at www.interscience.wiley.com.]

Discussion

In the present study, we have demonstrated that the expression levels of a candidate tumor suppressor gene termed *TSLC1* are significantly associated with unfavorable outcome of patients with neuroblastomas. Our array-CGH studies revealed that *TSLC1* gene locates within the SRO of deletion in primary neuroblastoma at 11q. Indeed, its expression levels in primary neuroblastomas correlated with several prognostic indicators for neuroblastoma such as stage, Shimada's pathological classification, *MYCN* amplification status, *TrkA* expression levels and DNA index. Furthermore, *TSLC1* had an ability to suppress neuroblastoma cell proliferation. Thus, it is likely that *TSLC1* acts as a putative tumor suppressor for neuroblastoma.

As described previously, loss of *TSLC1* expression in primary esophageal squamous cell carcinoma (ESCC) preferentially correlated with invasion and metastasis,¹² and a remarkable reduction of *TSLC1* expression levels was observed in primary lung adenocarcinomas with advanced stage.¹³ In addition, *TSLC1* expression was undetectable in 48% of benign (Grade I), 69% of atypical (Grade II) and 85% of anaplastic (Grade III) meningiomas.¹⁴ Consistent with these observations, a significant downregulation of *TSLC1* was seen in unfavorable neuroblastomas bearing *MYCN* amplification as compared with favorable ones carrying single copy of *MYCN*, indicating that the decreased expression levels of *TSLC1* is one of the general properties of various human tumors including neuroblastoma. Intriguingly, there might exist an inverse relationship between the expression levels of *TSLC1* and *MYCN* amplification status in primary neuroblastoma. Indeed, our immunohistochemical analysis demonstrated that *TSLC1* is detectable even in unfavorable neuroblastoma without *MYCN* amplification (Case 14). In a sharp contrast to primary neuroblastomas, the expression levels of *TSLC1* might be regulated in a *MYCN*-independent manner in neuroblastoma-derived cell lines. Although the precise molecular mechanisms behind the dysregulated expression of *TSLC1* in neuroblastoma cell lines, it might be due to certain genetic alterations occurred during the establishment of these cell lines.

Based on our present results, the presence of LOH at 11q was associated with unfavorable outcome of patients with neuroblastomas, however, there were no significant correlation between 11q LOH and the decreased expression levels of *TSLC1*. In accordance with these observations, the expression levels of *TSLC1* in neuroblastoma-derived cell lines were independent on their LOH status. These results suggest that the reduced expression levels of *TSLC1* in primary neuroblastomas are not attributed to haploinsufficiency. Alternatively, accumulating evidence strongly suggests that downregulation of *TSLC1* in various cancers including lung cancer, hepatocellular carcinoma, gastric cancer, pancreatic adenocarcinoma, prostate cancer, breast cancer, nasopharyngeal carcinoma

and cervical cancer, might be due to the hypermethylation of its promoter region.^{9,24-29} In a sharp contrast to these cancers, we did not detect the hypermethylation of the promoter region of *TSLC1* gene in primary neuroblastomas as well as neuroblastoma-derived cell lines under our experimental conditions. During the preparation of our article, Nowacki *et al.* found that there is no *TSLC1*-specific hypermethylation in neuroblastoma.³⁰ Similarly, the hypermethylation of *TSLC1* promoter region was not detectable in medulloblastoma.³¹ According to the previous results, *RASSF1A* and *CASP8* gene promoters were frequently hypermethylated in primary neuroblastoma and neuroblastoma cell lines.³² Thus, it is conceivable that, unlike the other cancers, hypermethylation of the promoter region of *TSLC1* does not contribute to its downregulation in neuroblastoma, and there might exist as yet unknown tissue-specific regulatory mechanisms of *TSLC1* transcription. Of note, the treatment of neuroblastoma-derived SH-SY5Y and CHP-134 cells with TSA (trichostatin A) resulted in a remarkable upregulation of *TSLC1*. Since TSA is a histone deacetylase inhibitor, it is likely that the acetylation status of histone plays an important role in the regulation of *TSLC1* expression. Further studies should be required to address this issue.

Several lines of evidence indicate that *TSLC1* has an ability to delay the cell cycle progression.^{12,16,33} Alternatively, enforced expression of *TSLC1* resulted in an activation of proapoptotic caspase-3 and induction of proteolytic cleavage of its substrate PARP.³⁴ These findings strongly suggest that *TSLC1* has an anti-proliferative and/or proapoptotic activity. In a good agreement with this notion, our present results demonstrated that enforced expression of *TSLC1* in SH-SY5Y cells as well as SK-N-AS cells decreases the number of drug-resistant colonies, and enforced depletion of the endogenous *TSLC1* in SH-SY5Y cells leads to an accelerated cell proliferation, which was consistent with the recent observations.³⁰ Collectively, our present findings suggest that *TSLC1* acts as a tumor suppressor for neuroblastoma, and also might contribute to the spontaneous regression of neuroblastoma arising from neuronal apoptosis and/or differentiation.

Acknowledgements

We thank institutions and hospitals for providing us tumor specimens. We are grateful to Drs. D.G. Albertson, D. Pinkel, B.G. Feuerstein, N. Tomioka, S. Oba and S. Ishii for their help to array CGH analysis. We also thank Mr. H. Kageyama, Dr. K. Koide, Dr. E. Isogai, Ms. N. Kitabayashi and Ms. Y. Nakamura for their excellent technical assistance. Dr. K. Ando is an awardee of Research Resident Fellowship from the Foundation for Promotion of Cancer Research (Japan) for the 3rd Term Comprehensive 10-Year Strategy for Cancer Control in Japan.

References

- Evans AE, Gerson J, Schnauer L. Spontaneous regression of neuroblastoma. *Natl Cancer Inst Monogr* 1976;44:49-54.
- Brodeur GM. Neuroblastoma: biological insights into a clinical enigma. *Nat Rev Cancer* 2003;3:203-16.
- Tomioka N, Oba S, Ohira M, Misra A, Fridlyand J, Ishii S, Nakamura Y, Isogai E, Hirata T, Yoshida Y, Todo S, Kaneko Y, et al. Novel risk stratification of patients with neuroblastoma by genomic signature which is independent of molecular signature. *Oncogene* 2008;27:441-9.
- Guo C, White PS, Weiss MJ, Hogarty MD, Thompson PM, Stram DO, Gerbing R, Matthay KK, Seeger RC, Brodeur GM, Maris JM. Allelic deletion at 11q23 in common in *MYCN* single copy neuroblastomas. *Oncogene* 1999;18:4948-57.
- Attiyeh EF, London WB, Mossé YP, Wang Q, Winter C, Khazi D, McGrady PW, Seeger RC, Look AT, Shimada H, Brodeur GM, Cohn SL, et al. Chromosome 1p and 11q deletions and outcome in neuroblastoma. *N Engl J Med* 2005;353:2243-53.
- Mossé Y, Greshock J, King A, Khazi D, Weber BL, Maris JM. Identification and high-resolution mapping of a constitutional 11q deletion in an infant with multifocal neuroblastoma. *Lancet Oncol* 2003;4:769-71.
- De Preter K, Vandesompele J, Menten B, Carr P, Fiegler H, Edsjö A, Carter NP, Yigil N, Waelput W, Van Roy N, Bader S, Pahlman S, et al. Positional and functional mapping of a neuroblastoma differentiation gene on chromosome 11. *BMC Genomics* 2005;6:97.
- Wang Q, Diskin S, Rappaport E, Attiyeh E, Mossé Y, Shue D, Seiser E, Jagannathan J, Shusterman S, Bansal M, Khazi D, Winter C, et al. Integrative genomics identifies distinct molecular classes of neuroblastoma and shows that multiple genes are targeted by regional alterations in DNA copy number. *Cancer Res* 2006;66:6050-62.
- Kuramochi M, Fukuhara H, Nobukuni T, Kanbe T, Maruyama T, Ghosh HP, Pletcher M, Isomura M, Onizuka M, Kitamura T, Sekiya T, Reeves RH, et al. *TSLC1* is a tumor suppressor gene in human non-small-cell lung cancer. *Nat Genet* 2001;27:427-30.
- Masuda M, Yageta M, Fukuhara H, Kuramochi M, Maruyama T, Nomoto A, Murakami Y. The tumor suppressor protein *TSLC1* is involved in cell-cell adhesion. *J Biol Chem* 2002;277:31014-19.
- Fukami T, Fukuhara H, Kuramochi M, Maruyama T, Isogai K, Sakamoto M, Takamoto S, Murakami Y. Promoter methylation of *TSLC1* gene in advanced lung tumors and various cancer cell lines. *Int J Cancer* 2003;107:53-9.
- Ito T, Shimada Y, Hashimoto Y, Kaganai J, Kan T, Watanabe G, Murakami Y, Imamura M. Involvement of *TSLC1* in progression of esophageal squamous cell carcinoma. *Cancer Res* 2003;63:6320-6.

13. Uchino K, Ito A, Wakayama T, Koma Y, Okada T, Ohbayashi C, Iseki S, Kitamura Y, Tsubota N, Okita Y, Okada M. Clinical implication and prognostic significance of the tumor suppressor *TSLC1* gene detected in adenocarcinoma of the lung. *Cancer* 2003;98:1002-7.
14. Surace EI, Lusic E, Murakami Y, Scheithauer BW, Perry A, Gutmann DH. Loss of tumor suppressor in lung cancer-1 (*TSLC1*) expression in meningioma correlates with increased malignancy grade and reduced patient survival. *J Neuropathol Exp Neurol* 2004;63:1015-27.
15. Houshmandi SS, Surace EI, Zhang HB, Fuller GN, Gutmann DH. Tumor suppressor in lung cancer-1 (*TSLC1*) functions as a glioma tumor suppressor. *Neurology* 2006;67:1863-6.
16. Lung HL, Cheung AK, Xie D, Cheng Y, Kwong FM, Murakami Y, Guan XY, Sham JS, Chua D, Protopopov AI, Zabarovsky ER, Tsao SW, et al. *TSLC1* is a tumor suppressor gene associated with metastasis in nasopharyngeal carcinoma. *Cancer Res* 2006;66:9385-92.
17. Brodeur GM, Pritchard J, Berthold F, Carlsen NL, Castel V, Castelberry RP, Bernardi BD, Evans AE, Favrot M, Hedborg F. Revisions of the international criteria for neuroblastoma diagnosis, staging, and response to treatment. *J Clin Oncol* 1993;11:1466-77.
18. Kaneko M, Tsuchida Y, Uchino J, Takeda T, Iwafuchi M, Ohnuma N, Mugishima H, Yokoyama J, Nishihira H, Nakada K, Sasaki S, Sawada T, et al. Treatment results of advanced neuroblastoma with the first Japanese study group protocol. Study Group of Japan for Treatment of Advanced Neuroblastoma. *J Pediatr Hematol Oncol* 1999;21:190-7.
19. Kaneko M, Nishihira H, Mugishima H, Ohnuma N, Nakada K, Kawa K, Fukuzawa M, Suita S, Sera Y, Tsuchida Y. Stratification of treatment of stage 4 neuroblastoma patients based on *N-myc* amplification status. *Med Pediatr Oncol* 1998;31:1-7.
20. Ohira M, Morohashi A, Imuzuka H, Shishikura T, Kawamoto T, Kageyama H, Nakamura Y, Isogai E, Takayasu H, Sakiyama S, Suzuki Y, Sugano S, et al. Expression profiling and characterization of 4200 genes cloned from primary neuroblastomas: identification of 305 genes differentially expressed between favorable and unfavorable subsets. *Oncogene* 2003;22:5525-36.
21. Misra A, Pellarin M, Shapiro J, Feuerstein BG. A complex rearrangement of chromosome 7 in human astrocytoma. *Cancer Genet Cytogenet* 2004;151:162-70.
22. Jain AN, Tokuyasu TA, Snijders AM, Segraves R, Albertson DG, Pinkel D. Fully automatic quantification of microarray image data. *Genome Res* 2002;12:325-32.
23. Kikuchi S, Yamada D, Fukami T, Maruyama T, Ito A, Asamura H, Matsuno Y, Onizuka M, Murakami Y. Hypermethylation of the *TSLC1/HGSF4* promoter is associated with tobacco smoking and a poor prognosis in primary non-small cell lung carcinoma. *Cancer* 2006;106:1751-8.
24. Fukuhara H, Kuramochi M, Fukami T, Kasahara K, Furuhashi M, Nobukuni T, Manyama T, Isogai K, Sekiya T, Shuin T, Kitamura T, Reeves RH, et al. Promoter methylation of *TSLC1* and tumor suppression by its gene product in human prostate cancer. *Jpn J Cancer Res* 2002;93:605-9.
25. Hoi AB, Lo KW, Kwong J, Lam EC, Chan SY, Chow LS, Chan AS, Teo PM, Huang DP. Epigenetic inactivation of *TSLC1* gene in nasopharyngeal carcinoma. *Mol Carcinog* 2003;38:170-8.
26. Honda T, Tamura G, Waki T, Jin Z, Sato K, Motoyama T, Kawata S, Kimura W, Nishizuka S, Murakami Y. Hypermethylation of the *TSLC1* gene promoter in primary gastric cancers and gastric cancer cell lines. *Jpn J Cancer Res* 2002;93:857-60.
27. Steenbergen RD, Kramer D, Braakhuis BJ, Stern PL, Verbeijen RH, Meijer CJ, Snijders PJ. *TSLC1* gene silencing in cervical cancer cell lines and cervical neoplasia. *J Natl Cancer Inst* 2004;96:294-305.
28. Jansen M, Fukushima N, Rosty C, Walter K, Altink R, Heck TV, Hruban R, Offerhaus JG, Goggins M. Aberrant methylation of 5' CpG island of *TSLC1* is common in pancreatic ductal adenocarcinoma and is first manifest in high-grade PanINs. *Cancer Biol Ther* 2002;1:293-6.
29. Allinen M, Peri L, Kujala S, Lahti-Domenici J, Outila K, Karpinen SM, Launonen V, Winqvist R. Analysis of 11q21-24 loss of heterozygosity candidate target genes in breast cancer: indications of *TSLC1* promoter hypermethylation. *Genes Chromosomes Cancer* 2002;34:384-9.
30. Nowacki S, Skowron M, Oberthuer A, Fagin A, Voth H, Brors B, Westermann F, Eggert A, Hero B, Berthold F, Fischer M. Expression of the tumor suppressor gene *TSLC1* is associated with favorable outcome and inhibits cell survival in neuroblastoma. *Oncogene* 2008;27:3329-38.
31. Lindsey JC, Lusher ME, Anderton JA, Bailey S, Gilbertson RJ, Pearson AD, Ellison DW, Clifford SC. Identification of tumor-specific epigenetic in medulloblastoma development by hypermethylation profiling. *Carcinogenesis* 2004;25:661-8.
32. Lázcoz P, Muñoz J, Nistal M, Pestaña A, Encio I, Castresana JS. Frequent promoter hypermethylation of *RASSF1A* and *CASP8* in neuroblastoma. *BMC Cancer* 2006;6:254.
33. Sussan TE, Pletcher MT, Murakami Y, Reeves RH. Tumor suppressor in lung cancer 1 (*TSLC1*) alters tumorigenic growth properties and gene expression. *Mol Cancer* 2005;4:28.
34. Mao X, Seidltz E, Truant R, Hitt M, Ghosh HP. Re-expression of *TSLC1* in a non-small-cell lung cancer cell line induces apoptosis and inhibits tumor growth. *Oncogene* 2004;23:5632-42.

KIF1B β Functions as a Haploinsufficient Tumor Suppressor Gene Mapped to Chromosome 1p36.2 by Inducing Apoptotic Cell Death^{*[S]}

Received for publication, March 25, 2008, and in revised form, June 9, 2008. Published, JBC Papers in Press, July 9, 2008, DOI 10.1074/jbc.M802316200

Arasambattu K. Munirajan^{1,5*}, Kiyohiro Ando², Akira Mukai², Masato Takahashi², Yusuke Suenaga², Miki Ohira², Tadayuki Koda³, Toru Hirota⁴, Toshinori Ozaki², and Akira Nakagawara^{1,5}

From the ¹Division of Biochemistry, Chiba Cancer Center Research Institute, Chiba 260-8717, Japan, ²Research Center for Functional Genomics, Hisamitsu Pharmaceutical Company, Inc., Tokyo 141-8577, Japan, the ³Department of Genetics, Dr. ALM PG Institute of Basic Medical Sciences, University of Madras, 600-113 Chennai (Madras), India, and the ⁴Department of Experimental Pathology, The Cancer Institute, Tokyo 135-8550, Japan

Deletion of the distal region of chromosome 1 frequently occurs in a variety of human cancers, including aggressive neuroblastoma. Previously, we have identified a 500-kb homozygously deleted region at chromosome 1p36.2 harboring at least six genes in a neuroblastoma-derived cell line NB1/C201. Among them, only KIF1B β , a member of the kinesin superfamily proteins, induced apoptotic cell death. These results prompted us to address whether KIF1B β could be a tumor suppressor gene mapped to chromosome 1p36 in neuroblastoma. Hemizygous deletion of KIF1B β in primary neuroblastomas was significantly correlated with advanced stages ($p = 0.0013$) and MYCN amplification ($p < 0.001$), whereas the mutation rate of the KIF1B β gene was infrequent. Although KIF1B β allelic loss was significantly associated with a decrease in KIF1B β mRNA levels, its promoter region was not hypermethylated. Additionally, expression of KIF1B β was markedly down-regulated in advanced stages of tumors ($p < 0.001$). Enforced expression of KIF1B β resulted in an induction of apoptotic cell death in association with an increase in the number of cells entered into the G₂/M phase of the cell cycle, whereas its knockdown by either short interfering RNA or by a genetic suppressor element led to an accelerated cell proliferation or enhanced tumor formation in nude mice, respectively. Furthermore, we demonstrated that the rod region unique to KIF1B β is critical for the induction of apoptotic cell death in a p53-independent manner. Thus, KIF1B β may act as a haploinsufficient tumor suppressor, and its allelic loss may be involved in the pathogenesis of neuroblastoma and other cancers.

10% of all pediatric cancers (1). Neuroblastomas are derived from sympathetic neuroblasts with various clinical outcomes from spontaneous regression because of neuronal differentiation and/or apoptotic cell death to malignant progression. Extensive cytogenetic and molecular genetic studies identified that genetic abnormalities such as loss of short arm of chromosome 1 (1p), amplification of MYCN, and 17q gain are frequently observed and often associated with poor clinical outcome (2, 3). The actual prevalence of 1p deletion in neuroblastoma is ~35% (4–9). The deleted regions were extensively mapped to identify the candidate tumor suppressor gene(s) that has been deleted out from this region (10–17). A chromosomal locus 1p36 is frequently deleted in aggressive neuroblastoma, pheochromocytoma, colon, liver, brain, breast, and other cancers (18, 19). Transfer of 1p chromosome segments into neuroblastoma-derived cell line NGP.1A.TR1 resulted in a significant suppression of their tumor formation (20). Furthermore, previous studies indicated that there is no single site of deletion on the distal part of 1p36, but there are at least three discrete regions that are commonly deleted in neuroblastoma, indicating that they may harbor potential tumor suppressor gene(s) (8).

Tumor suppressor genes, one of the main classes of cancer-associated genes, encode inhibitors of cell proliferation and/or activators of apoptotic cell death and are involved in a variety of molecular mechanisms behind cell growth suppression (21). Tumor suppressor genes frequently mutated in other malignancies do not appear to play a major role in the generation of neuroblastoma, indicating that development of this type of tumor employs one or more previously unidentified genetic pathways. To date, a majority of candidate tumor suppressor genes has been identified by mapping the minimal deleted region and searching for the intact homologous region of mutated genes. This experimental strategy fails when the second allele is silenced by promoter hypermethylation or the targeted gene is haploinsufficient for tumor suppression, a situation where loss of one allele confers a selective advantage for tumor growth. Several examples of such haploinsufficiency for tumor suppression have been demonstrated in the case of p27^{KIP1}, p53, and PTEN (22, 23).

We and other investigators have previously identified a 500-kb homozygous deletion at 1p36.2 harboring at least six

Neuroblastoma is one of the most common malignant solid tumors occurring in infancy and childhood and accounts for

* This work was supported by the Ministry of Education, Culture, Sports, Science and Technology of Japan and the Ministry of Health, Labor and Welfare of Japan. The costs of publication of this article were defrayed in part by the payment of page charges. This article must therefore be hereby marked "advertisement" in accordance with 18 U.S.C. Section 1734 solely to indicate this fact.

[S] The on-line version of this article (available at <http://www.jbc.org>) contains supplemental Figs. S1–S5.

¹ To whom correspondence should be addressed: Division of Biochemistry, Chiba Cancer Center Research Institute, 666-2 Nitona, Chuo-ku, Chiba 260-8717, Japan. Tel.: 81-43-264-5431; Fax: 81-43-265-4459; E-mail: akiranak@chiba-cc.jp.

genes, *PEX14*, *UFD2a*, *KIF1B*, *CORT*, *DFF45*, and *PGD*, in a neuroblastoma-derived cell line NB1/C201 (12, 15, 24). In this study, we have demonstrated that only *KIF1B*, a member of the kinesin 3 family genes (25), might be a tumor suppressor gene mapped to chromosome 1p36 in neuroblastoma. Kinesins are microtubule-dependent intracellular motors involved in the transport of organelles, vesicles, protein complexes, and RNA to specific destinations (26, 27). *KIF1B* encodes two alternatively spliced isoforms, including *KIF1B α* and *KIF1B β* , and both form homodimers and transport mitochondria and synaptic vesicle precursors, respectively (28). The NH₂-terminal motor domain of *KIF1B α* is identical to *KIF1B β* , whereas COOH-terminal tails share no structural homology. A point mutation in the ATP-binding site within the motor domain of *KIF1B β* has been closely linked to Charcot-Marie Tooth disease type 2A (29).

In this study, we cloned a full-length *KIF1B β* cDNA, generated recombinant adenovirus encoding *KIF1B β* , and examined its biological role in neuroblastoma and other cell lines. We systematically analyzed *KIF1B β* for LOH,² mutation, and promoter methylation. Our genetic and functional analyses clearly showed that *KIF1B β* is a tumor suppressor, although not a classic one. *KIF1B β* might act as a haploinsufficient tumor suppressor, and its down-regulation might potentially contribute to tumorigenesis of cancers, including neuroblastoma.

EXPERIMENTAL PROCEDURES

Cell Lines and Tumor Samples—Human neuroblastoma (NB) cell lines such as SH-SY5Y, NB1, and SK-N-BE were grown in RPMI 1640 medium supplemented with heat-inactivated fetal bovine serum, 100 units/ml penicillin, and 100 μ g/ml streptomycin. NMuMG, COS7, HEK293, and HeLa cells were grown in Dulbecco's modified Eagle's medium containing 10% heat-inactivated fetal bovine serum, 100 units/ml penicillin, and 100 μ g/ml streptomycin. Tumor DNA and RNA samples were obtained from our Neuroblastoma Resource Bank. Informed consent was obtained at each hospital.

GSE-mediated Tumor Formation in Nude Mice—GSE assay was performed as described previously (30). In brief, a cDNA fragment (nucleotide number 2658–3115 of GenBankTM accession number AB017133) corresponding to the unique region of *KIF1B β* was amplified by PCR-based strategy and subcloned into the HpaI site of the pLXSN vector in an antisense orientation to give pLXSN-antisense *KIF1B β* . NMuMG mammary gland cells (1×10^6 cells) infected with pLXSN or with pLXSN-antisense *KIF1B β* were inoculated subcutaneously into the femoral region of nude mice. In the experiments using live animals, we strictly followed the Chiba Cancer Center Research Institute guidelines and protocols for handling live animals.

Construction of Expression Plasmids and Recombinant Adenovirus—*KIF1B β* splicing variants I, III, and IV fused to the FLAG epitope at their NH₂ termini were amplified by PCR

KIF1B β Is a Haploinsufficient Tumor Suppressor

using cDNA prepared from CHP134 cells as a template and subcloned into pcDNA3.1 (Invitrogen). *KIF1B β* -GFP deletion constructs were produced by PCR-based amplification. The recombinant adenovirus was constructed as described previously (31). Briefly, *KIF1B β* cDNA was subcloned into pHMCMV6 adeno-shuttle vector. The shuttle vector was then digested with I-Ceu I and P1-Sce I and inserted into the identical restriction sites of the adenovirus expression vector pAdHM4. All of the recombinant vectors were verified by DNA sequencing. Recombinant adenoviruses were produced by transfecting the PacI-digested expression constructs into HEK293 cells. An expression vector encoding GFP was used to monitor the efficiency of infection.

Mutation Analysis—For the detection of *KIF1B β* mutations, we designed primer sets covering the motor domain and 2 kb of the 5'-upstream region of *KIF1B β* . After PCR-based amplification, PCR products were separated by 5% nondenaturing polyacrylamide gels. After electrophoresis, PCR products were gel-purified and subcloned into pGEM-T Easy Vector (Promega), and their DNA sequences were determined by an automated DNA sequencer (Applied Biosystems).

Flow Cytometry—Cells were fixed in ice-cold 70% ethanol, treated with 50 mM sodium citrate, 100 μ g/ml RNase A, 50 μ g/ml propidium iodide and subjected to FACS analysis (BD Biosciences) according to the manufacturer's instructions.

Construction of *KIF1B β* siRNA Expression Vector—An siRNA expression vector termed pMuniH1, in which the cytomegalovirus promoter of pcDNA 3.1 was replaced with the H1 promoter, was generated. Sense and antisense oligonucleotides for *KIF1B β* (nucleotide number 371–389 of GenBankTM accession number AB017183) were joined by a 9-base loop, annealed, and subcloned into pMuniH1.

Luciferase Reporter Assay—The genomic fragments corresponding nucleotide positions –887/+106, –630/+106, and –294/+106 of the *KIF1B β* gene were amplified from human placenta genomic DNA and cloned into pGL3-Basic luciferase reporter plasmid (Promega) to give pGL3(–887/+106), pGL3(–630/+106), and pGL3(–294/+106). For luciferase assay, SK-N-BE cells were transfected with pRL-TK (Promega) encoding *Renilla* luciferase cDNA and the indicated luciferase reporter constructs. Forty eight hours after transfection, firefly and *Renilla* luciferase activities were measured by dual-luciferase reporter assay system (Promega), and firefly luciferase activity was normalized to *Renilla* luciferase activity.

Methylation-specific PCR—The methylation status of the promoter region of *KIF1B β* was assessed by methylation-specific PCR as described previously (32).

Cell Cycle Analysis—Cells were fixed in 3.7% formaldehyde and permeabilized with 0.2% Triton X-100 and DNA was stained with 0.1 μ g/ml of 4',6'-diamidino-2-phenylindole. Cellular DNA content was analyzed by laser scanning cytometry (LSC2 System, Olympus).

Array-CGH Analysis—Array CGH analysis of 112 sporadic primary neuroblastomas using a chip carrying 2,464 bacterial artificial chromosome clones was conducted as described previously (33). All array-CGH data are available at NCBI Gene Expression Omnibus (GEO, www.ncbi.nlm.nih.gov) with accession number GSE 5784.

² The abbreviations used are: LOH, loss of heterogeneity; CGH, comparative genomic hybridization; FHA, forkhead-associated; GSE, genetic suppressor element; KIF, kinesin superfamily protein; NB, neuroblastoma; NGF, nerve growth factor; FACS, fluorescence-activated cell sorter; siRNA, short interfering RNA; MTT, 3-(4,5-dimethylthiazol-2-yl)-2,5-diphenyltetrazolium bromide; RT, reverse transcription; GFP, green fluorescent protein.

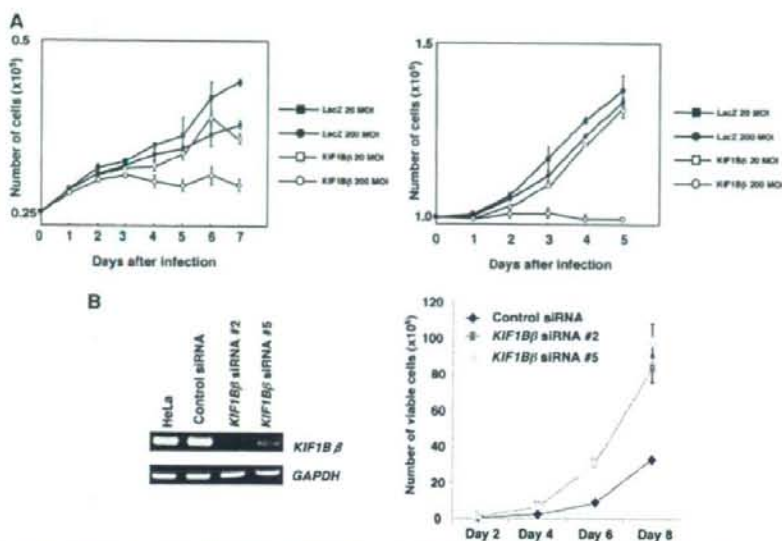
KIF1B β Is a Haploinsufficient Tumor Suppressor

FIGURE 1. KIF1B β has a growth-suppressive activity *in vitro*. **A**, NB1 (left panel) and NMuMG (right panel) cells were infected with recombinant adenovirus encoding LacZ or KIF1B β at the indicated multiplicity of infection (MOI). At the indicated time points after infection, the number of viable cells was measured. **B**, HeLa cells stably expressing control siRNA-2 or siRNA-5 against KIF1B β were established, and the expression levels of the endogenous KIF1B β were examined by RT-PCR (left panel). Glyceraldehyde-3-phosphate dehydrogenase (GAPDH) was used as an internal control. Number of viable cells was measured at the indicated time points (right panel).

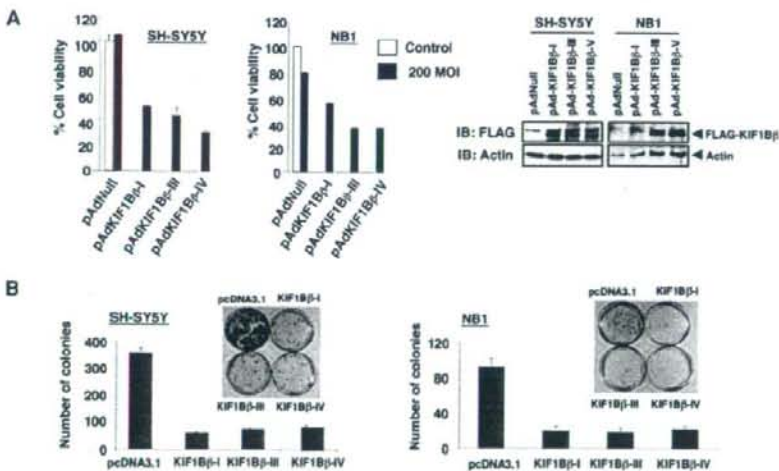


FIGURE 2. Enforced expression of KIF1B β induces growth suppression in neuroblastoma-derived cell lines. **A**, MTT assay. Neuroblastoma-derived SH-SY5Y and NB1 cells were infected with the indicated recombinant adenoviruses, including empty adenovirus (pAdNull) at a 200 multiplicity of infection (MOI) (filled boxes) or left untreated (open boxes). Twenty four hours after infection, infected SH-SY5Y and NB1 cells were seeded at a density of 1×10^3 cells/96-well plates and allowed to attach. Ninety six hours after infection, 10 μ l of MTT solution was added to each well and incubated for 3 h at 37 $^{\circ}$ C (left panel). Right panels show the expression of the indicated splicing variants of KIF1B β as examined by immunoblotting (IB) with anti-FLAG antibody. **B**, colony formation assay. SH-SY5Y and NB1 cells were transfected with an empty plasmid or with the indicated expression plasmids. Forty eight hours after transfection, cells were transferred into fresh medium containing 500 μ g/ml of G418 and incubated for 2 weeks. After selection with G418, G418-resistant viable colonies were stained with Giemsa solution, and number of colonies was scored.

Caspase Assay—Caspase activity was measured by using caspase-3/7 assay system (Promega) according to the manufacturer's instructions.

Statistics—The Student's *t* test was used as a statistical method. Statistical significance was declared if the *p* value was <0.05 .

RESULTS

Identification of KIF1B β as a Candidate Tumor Suppressor Mapped to Chromosome 1p36.2—To search for a candidate tumor suppressor gene(s), we first transferred each of the above-mentioned six genes into NB1 and nontransformed NMuMG mouse epithelial cells (30), and we found that only KIF1B β induces growth suppression in a dose-dependent manner (Fig. 1A). In contrast, our preliminary observations indicated that its alternative splicing variant KIF1B α lacking a COOH-terminal rod region has marginal effects on cell growth in NB1 cells (data not shown). In support of these results, siRNA-mediated knockdown of KIF1B β in HeLa cells without 1p loss markedly enhanced their cell growth (Fig. 1B). In addition, enforced expression of KIF1B β induced growth retardation in p53-deficient H1299 cells and HeLa cells in which p53 is inactivated because of the presence of E6-AP (data not shown).

Overexpression of KIF1B β in Neuroblastomas-induced Apoptotic Cell Death—During PCR-based screening of human KIF1B β cDNA from human neuroblastoma cell lines, we identified at least four splicing variants that lacked exons 14 and/or 15 (supplemental Fig. S1). Similar splicing variants have also been observed in mice and rats (34). We successfully generated recombinant adenoviruses for human KIF1B β -I, -II, and -IV variants (Fig. 2A). Enforced expression of these splicing variants promoted apoptotic cell death in both SH-SY5Y (without 1p loss) and NB1 neuroblastoma cell lines as determined by MTT and FACS analyses (Fig. 2A and supplemental Fig. S2). Consistent with these results, colony formation assay showed that all these KIF1B β splicing variants strongly reduced the number of drug-resistant colonies in SH-SY5Y and NB1 neuroblastoma cells (Fig. 2B). These findings suggest that multiple KIF1B β splicing isoforms

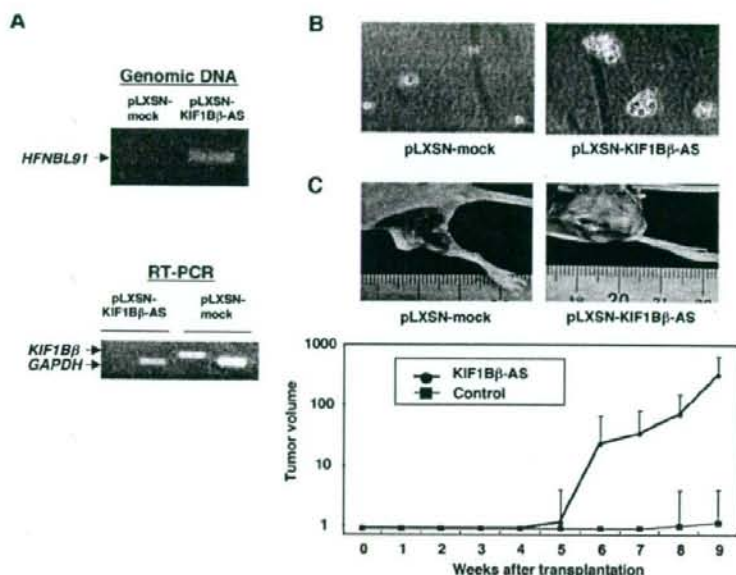
KIF1B β Is a Haploinsufficient Tumor Suppressor

FIGURE 3. Tumor formation *in vivo*. A, NMuMG cells were infected with an empty retrovirus vector (pLXSN) or with pLXSN bearing mouse antisense *KIF1B β* (pLXSN-KIF1B β -AS). Genomic integration of the antisense *KIF1B β* was examined by PCR (upper panel). Lower panel shows the expression levels of *KIF1B β* as examined by RT-PCR. Arrows indicate the positions of PCR products corresponding to *KIF1B β* and *GAPDH*. B, NMuMG cells (5×10^6 cells) infected with pLXSN or pLXSN-KIF1B β -AS were suspended in 3 ml of 0.4% low melting agarose dissolved in culture medium, plated onto agarose bed consisting of 0.8% low-melting agarose, and incubated at 37 °C for 5 weeks. C, tumor formation in nude mice. NMuMG cells (1×10^6 cells) infected with the indicated retroviruses were injected subcutaneously and tumor volumes were estimated weekly (lower panel). Upper panels show tumors generated in nude mice.

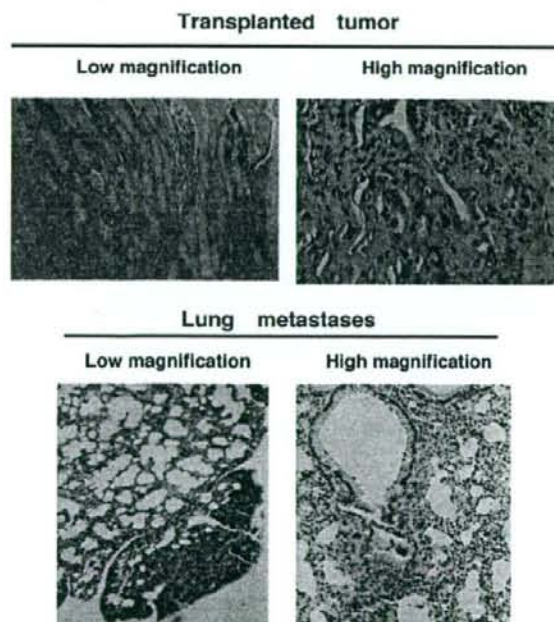


FIGURE 4. Histology of tumors generated in nude mice. Representative photographs of tumors (upper panels) and lung metastases (lower panels) are shown. For histological analyses, tumor tissues were removed from animals and immediately fixed in 10% formaldehyde and embedded in paraffin, and 3- μ m sections were stained with hematoxylin and eosin.

possess tumor suppressor activity. Intriguingly, the expression pattern of *KIF1B β* splicing variants was varied among various human tissues (supplemental Fig. S3).

Knockdown of *KIF1B β* Expression Accelerates Growth of NMuMG Cells and Tumor Formation in Nude Mice—We then asked whether genetic disruption of *KIF1B β* gene could be critical for tumorigenesis. For this purpose, we employed a genetic suppressor element (GSE) strategy (30). A mouse genomic DNA corresponding to a *KIF1B β* cDNA fragment (nucleotide number 2658–3115 of GenBank™ accession number AB017133) encoding the unique region of *KIF1B β* was subcloned into the retrovirus pLXSN vector in an antisense orientation to give pLXSN-KIF1B β -AS. NMuMG cells, immortalized mouse mammary gland cells, stably infected with pLXSN-KIF1B β -AS, showed more than 80% reduction in endogenous *KIF1B β* expression (Fig. 3A) and formed significantly larger colonies than empty vector-infected control cells

in soft agar medium (Fig. 3B). In addition, all eight mice subcutaneously transplanted with NMuMG cells stably infected with pLXSN-KIF1B β -AS displayed remarkable tumor growth (Fig. 3C). On the other hand, only two of eight mice transplanted with the empty vector-infected cells formed tumors, which were smaller in both cases (note log scale in Fig. 3C). The tumors formed by cells lacking *KIF1B β* expression were histologically diagnosed as poorly differentiated invasive ductal carcinoma and frequently metastasized to the lung (Fig. 4). Thus, it is likely that *KIF1B β* exerts tumor-suppressive function *in vivo*.

LOH of *KIF1B β* Locus Is Frequently Observed in Primary Advanced Neuroblastomas—We next sought to search for LOH at chromosome 1p36 in 112 sporadic neuroblastomas using array-based comparative genomic hybridization (array-CGH). Similar to previous reports, the smallest region of overlap at the distal region of chromosome 1p identified in 37 primary neuroblastomas with 1p loss was between 1p36.22 and 1pter and included *KIF1B*, *CHD5*, *TP73*, and *SKI* (supplemental Fig. S4). Thirty two percent (30/95) of neuroblastomas examined had lost one *KIF1B β* allele as determined by quantitative real time genomic PCR (Table 1). *KIF1B β* was hemizygously deleted in 18% of early neuroblastomas (stages 1 and 2, $n = 51$), in 55% of advanced neuroblastomas (stages 3 and 4, $n = 38$) ($p = 0.0013$), in 13% of primary neuroblastomas with a single copy of *MYCN* ($n = 70$), and in 84% of *MYCN*-amplified primary neuroblastomas ($n = 25$) ($p < 0.001$). No homozygous deletion was detected in the primary tumors examined.

KIF1B Is a Haploinsufficient Tumor Suppressor

Decreased Expression of KIF1B Is Associated with Monoallelic Loss of the Gene in Primary Neuroblastomas—We examined expression levels of KIF1B mRNA in 102 primary neuroblastomas by using both semi-quantitative and quantitative real time PCR. As shown in Fig. 5, A and B, expression levels of KIF1B mRNA were significantly higher in tumors at favorable stages (1, 2, and 4s, 1.654 ± 0.257 , mean \pm S.E., $n = 60$) than in those at advanced stages (3 and 4, 0.503 ± 0.180 , $n = 42$, $p < 0.001$). To address whether its expression levels could be correlated with number of alleles at the KIF1B gene locus, we examined primary tumors with a diploid karyotype. As shown in the

lower panel of Fig. 5B, tumors with monoallelic loss of KIF1B gene locus expressed significantly lower levels of KIF1B mRNA (0.126 ± 0.092 , $n = 13$) as compared with those with two KIF1B alleles (0.364 ± 0.035 , $n = 16$, $p = 0.019$). These results suggest that KIF1B is a haploinsufficient tumor suppressor gene in high risk neuroblastomas.

No Promoter Methylation and Rare Mutations Are Observed in Neuroblastoma Cell Lines and Primary Neuroblastomas—Our initial mutation searches of KIF1B gene were focused on its motor domain and the proximal (~2 kb) promoter region in 21 primary neuroblastomas with 1p36 LOH and in 17 neuroblastoma cell lines. As shown in Table 2, we identified only a silent mutation GCC-GCG (at codon 95) in two primary tumors, a 2-bp (CC) deletion (at -113/-114) and G-A base change (at -336) in the KIF1B promoter region in three primary tumors and four neuroblastoma cell lines. Because these aberrations were also found in the control samples, it is likely that these base changes reflect single nucleotide polymorphisms of the Japanese population.

To further extend our mutation searches, we have examined the presence or absence of KIF1B mutations within its whole coding region in 100 primary neuroblastoma tissues. Finally, we found out the missense mutations (N737S) in six independent cases. However, their functional significances remained unclear.

Methylation of CpG islands in the promoters has been considered to be another well recognized molecular mechanism behind the inactivation of the tumor suppressor gene. To determine whether the methylation of CpG island could contribute to the inactivation of KIF1B, the region spanning exon 1 and 5'-upstream sequences (nucleotide number -877 to +106) of KIF1B was cloned and analyzed for promoter activity by luciferase reporter assay. As shown in Fig. 6, A and B, KIF1B promoter region existed at nucleotide position between -630 and -294. We then identified KIF1B CpG islands within the promoter region and investigated whether these CpGs could be methylated in primary neuroblastomas as well as cell lines. The methylation-specific PCR analysis demonstrated that all of the CpG clusters are unmethylated, suggesting that KIF1B is not inactivated by methylation (Fig. 6C).

The COOH-terminal Region between FHA and Pleckstrin Homology Domains of KIF1B Is Responsible to Induce Apoptotic Cell Death—To map a critical domain(s) of KIF1B responsible for its tumor-suppressive function, we generated NH₂-

TABLE 1

Frequency of LOH of the KIF1B gene

LOH was examined by both array-CGH and quantitative real time PCR using genomic DNA obtained from primary neuroblastomas (tumor cells component, >70%). The cutoff value of the LOH score was 0.8 in the latter.

| Category | n | KIF1B LOH | |
|---------------|----|-----------|----|
| | | LOH (+) | % |
| Stage | | | |
| 1 | 36 | 6 | 17 |
| 2 | 15 | 3 | 20 |
| 3 | 7 | 3 | 43 |
| 4 | 31 | 18 | 58 |
| 4s | 6 | 0 | 0 |
| MYCN | | | |
| Single copy | 70 | 9 | 13 |
| Amplification | 25 | 21 | 84 |
| Total | 95 | 30 | 32 |

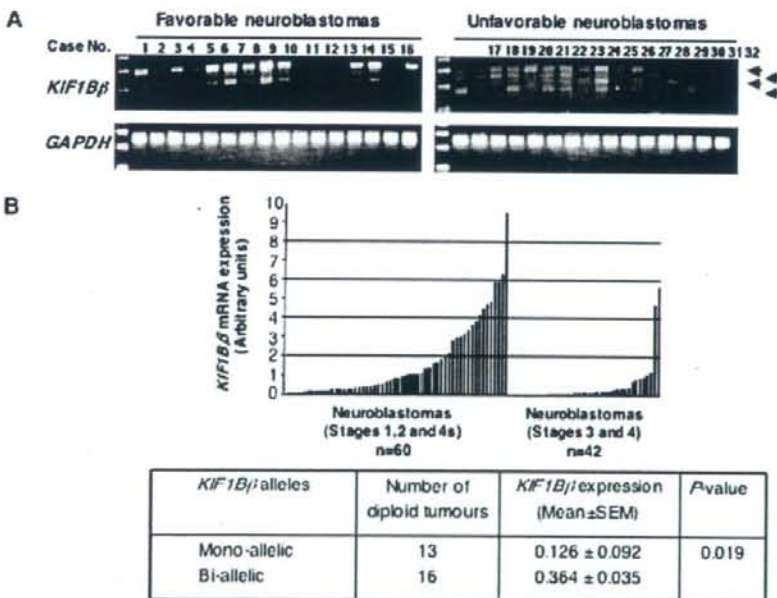


FIGURE 5. Expression levels of KIF1B in primary neuroblastomas. A, semi-quantitative RT-PCR analysis. Total RNA was prepared from favorable ($n = 16$; stages 1 and 2, MYCN single copy) and unfavorable ($n = 16$; stages 3 and 4, MYCN amplified) neuroblastomas and subjected to semi-quantitative RT-PCR to examine the expression levels of KIF1B. Glyceraldehyde-3-phosphate dehydrogenase (GAPDH) was used as an internal control. B, quantitative real time PCR. Expression levels of KIF1B were standardized using the corresponding glyceraldehyde-3-phosphate dehydrogenase value of each neuroblastoma sample. The relative expression levels of KIF1B in favorable (stages 1, 2, and 4s) and advanced (stages 3 and 4) neuroblastomas are shown (upper panel). Lower panel shows a significant correlation between mono-allelic loss of KIF1B gene and its lower expression levels.

KIF1B β Is a Haploinsufficient Tumor Suppressor

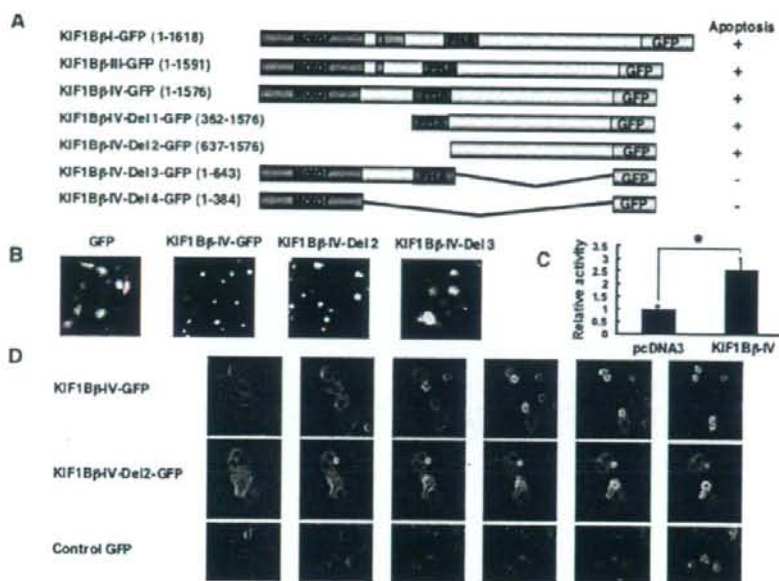


FIGURE 7. The coiled-coil region is required for KIF1B β -mediated apoptotic cell death. *A*, schematic representation of GFP-tagged KIF1B β deletion mutants and summary of their ability to induce apoptotic cell death. *B*, COS7 cells were transiently transfected with the indicated expression plasmids. Forty eight hours after transfection, morphologies of GFP-positive cells were examined by a confocal laser scanning microscope. *C*, caspase activity. HeLa cells were transiently transfected with the indicated expression plasmids. Forty eight hours after transfection, cell lysates were prepared, and their caspase activities were measured. Statistically significant differences are indicated by asterisks ($p < 0.05$). *D*, time course experiments. The indicated expression plasmids were transiently introduced into COS7 cells. Forty eight hours after transfection, changes of morphology of GFP-positive cells were monitored for 12 h.

domain (with or without FHA domain) also induced apoptotic cell death. In contrast, expression of KIF1B β mutants lacking the COOH-terminal rod domain did not promote apoptotic cell death (Fig. 7, *A* and *B*). Under our experimental conditions, enforced expression of KIF1B β variant-IV resulted in a significant increase in the caspase activities (Fig. 7*C*), suggesting that KIF1B β -mediated apoptotic cell death might be regulated in a caspase-dependent manner. Our further analysis using other deletion mutants revealed that the 807 amino acids death-inducing region is located between FHA and pleckstrin homology domains (data not shown).

To determine whether the kinesin activity of KIF1B β could be necessary for its tumor-suppressive function, we introduced a Q98L mutation within a consensus ATP-binding site of KIF1B β -IV splicing variant (Fig. 8*A*). This mutation disrupts the motor function of KIF1B β (29). In addition, a KIF1B β -IV splicing variant carrying two point mutations (Q560A and D568A) within its highly conserved amino acid residues of FHA domain, which may be critical for binding to Ser/Thr-phosphorylated motifs of the interacting proteins, was also generated. In addition to these two mutants, we also generated an additional mutant bearing Q98L, Q560A, and D568A. These three mutants, however, retained an ability to induce apoptotic cell death, suggesting that KIF1B β -mediated apoptotic cell death does not require its ability to transport cargo using its motor domain (Fig. 8*B*).

detectable in this study, several losses of function mutations in the coding region of KIF1B β gene in a large number of primary neuroblastomas, pheochromocytomas, and medulloblastomas have now been identified.³ Homozygous deletion of KIF1B in mice resulted in death just after birth because of apnea. However, heterozygous mice are viable with a phenotype resembling Charcot-Marie-Tooth disease type 2A (29). To date, no information has been available in the literature regarding spontaneous tumor formation in KIF1B-heterozygous mice. It is possible that these mice have not been followed long enough or that loss of one KIF1B allele is not sufficient for tumor formation and requires cooperating mutations for spontaneous tumor formation. Since there is functional disruption of wild-type p53 because of its mislocalization, haploinsufficiency of the KIF1B β gene might contribute to tumorigenesis of aggressive neuroblastomas with 1p LOH and MYCN amplification (37). KIF1B β might also be involved in tumorigenesis in combination with other contiguous 1p36.3 genes such as p73 (38) and CHD5 (39).

Finally, we have identified four different splicing variants of KIF1B β . However, colony formation assay revealed that all of the splicing variants almost equally suppress cell growth, indicating that its tumor-suppressive function may not be dependent on alternative splicing events. The deletion construct termed Del 2-GFP encoding amino acid residues 637–1576

³ S. Schlisio and W. G. Kaelin, Jr., personal communication.

DISCUSSION

In this study, we have shown that the KIF1B β gene is hemizygotously deleted especially in aggressive primary neuroblastoma tumors, and its mutation is infrequent. The expression of KIF1B β was kept at quite a low level in aggressive neuroblastoma subsets, even though no methylation of its promoter region was observed. One of the well known haploinsufficient tumor suppressors is the cyclin-dependent kinase inhibitor p27^{KIP1} (35). The heterozygous mice of p27^{KIP1} developed tumors when mice were treated with tumor-promoting agents, and tumors retained the normal p27^{KIP1} allele. Additionally, hemizygotous loss of p27^{KIP1} and/or reduced expression level of p27^{KIP1} conferred poor prognosis in human cancers (36). Taken together, our present results suggest that, like p27^{KIP1}, KIF1B β is a haploinsufficient tumor suppressor gene of neuroblastoma, and its function to induce apoptotic cell death is regulated in a p53-independent manner. Although homozygous deletion or mutations of KIF1B β were rarely

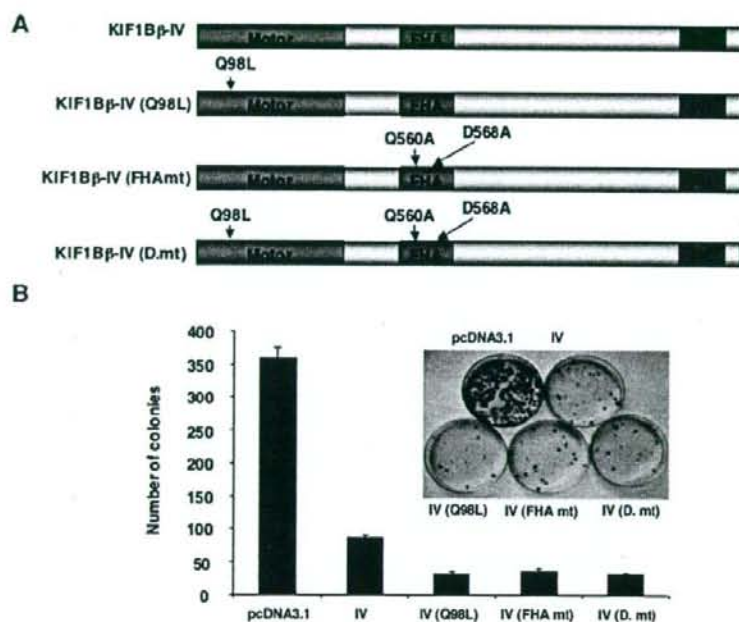
KIF1B β Is a Haploinsufficient Tumor Suppressor

FIGURE 8. Motor and FHA domains are not required for KIF1B β -mediated growth suppression. *A*, schematic drawing of mutant forms of KIF1B β . Point mutations (Q98L, Q560A, and D568A) were introduced into KIF1B β by using the QuickChange XL site-directed mutagenesis kit (Stratagene) following the manufacturer's recommendations. *B*, colony formation assay. SH-SY5Y cells were transfected with an empty vector or with the indicated expression vectors. Forty eight hours after transfection, cells were transferred into fresh medium containing 500 μ g/ml of G418. Two weeks after selection, G418-resistant colonies were fixed and stained with Giemsa solution, and number of drug-resistant colonies was scored.

induced apoptotic cell death similar to wild-type KIF1B β . Therefore, this region containing two predicted coiled-coils (amino acid residues 668–737 and 841–863) alone is sufficient for pro-apoptotic function of KIF1B β . The coiled-coil motifs are amphipathic oligomerization motifs. The tumor suppressor par-4 with a potential coiled-coil structure induced apoptotic cell death in prostate cancer cell lines (40, 41). Moreover, a putative coiled-coil domain of potential tumor suppressor protein, Prohibitin, has been shown to be sufficient to repress E2F1-mediated transcription and induction of apoptotic cell death (42).

In neuroblastoma, polyploidy is very common, which is often associated with a better prognosis. The precise molecular mechanisms underlying this phenomenon still remain unclear. Recently, defects in mitotic spindle check point gene products such as MAD1, MAD2, BUB1, BUB3, and BUBR1 have been implicated in the generation of polyploidy (43). Intriguingly, attached cells expressing GFP-tagged KIF1B β splicing variants exhibited a perturbation of G₂/M progression and multinucleation (supplemental Fig. S5). The precise molecular mechanisms by which KIF1B β could promote these cellular abnormalities and apoptotic cell death are currently unknown. On the other hand, down-regulation of KIF1B β resulted in augmented cell proliferation *in vitro* and tumor formation *in vivo*, indicating that KIF1B β might have a critical role in the regulation of mitosis like other mitotic kinesins (44). It is conceivable that KIF1B β might act in a dominant inhibitory manner to

sequester fundamental cytoplasmic factors that are required for proper cell cycle progression. In this connection, we are undertaking to identify the KIF1B β -binding partner(s), which might clarify the molecular mechanisms behind growth suppression and/or apoptotic cell death mediated by KIF1B β .

The nerve growth factor (NGF) dependence of tumor cells through the TrkA-p75^{NTR} receptor complex plays a critical role in the regulation of the spontaneous regression and differentiation in neuroblastoma (45). NGF depletion-induced apoptotic cell death is blocked in aggressive neuroblastoma (46). The findings showing that expression of KIF1B β also increases during apoptotic cell death triggered by NGF depletion in PC12 cells³ strengthen the significance of the tumor suppressor function of KIF1B β in primary neuroblastomas and pheochromocytoma. Indeed, some kinesin family proteins are involved in the regulation of apoptotic cell death in developing neurons (47). In conclusion, our present results unveiled that

KIF1B β , mapped to chromosome 1p36.2, is the candidate tumor suppressor gene of the kinesin family functioning in a manner of haploinsufficiency.

Acknowledgments—We thank Hajime Kageyama for help in FACS analysis and DNA sequencing; Yuki Nakamura, Natsue Kitabayashi, and Ayaka Nobusato for their excellent technical assistance; Drs. Keizo Takenaga, Kou Miyazaki, Hisashi Tokita, Nobumoto Tomioka, Yoko Nakamura, and Daihachiro Tomotsune for helpful discussions; and Drs. E. Thavathiru and Margaret Das for critical reading of the manuscript.

REFERENCES

- Westermann, F., and Schwab, M. (2002) *Cancer Lett.* **184**, 127–147
- Brodeur, G. M., Seeger, R. C., Schwab, M., Varmus, H. E., and Bishop, J. M. (1984) *Science* **224**, 1121–1124
- Caron, H. (1995) *Med. Pediatr. Oncol.* **24**, 215–221
- Gehring, M., Berthold, R., Edler, L., Schwab, M., and Amler, L. C. (1995) *Cancer Res.* **55**, 5366–5369
- White, P. S., Maris, J. M., Beltinger, C., Sulman, E., Marshall, H. N., Fujimori, M., Kaufman, B. A., Biegel, J. A., Allen, C., Hilliard, C., Valentine, M. B., Look, A. T., Enomoto, H., Sakiyama, S., and Brodeur, G. M. (1995) *Proc. Natl. Acad. Sci. U. S. A.* **92**, 5520–5524
- Martinsson, T., Sjöberg, R. M., Hedberg, F., and Kongner, P. (1995) *Cancer Res.* **55**, 5681–5686
- White, P. S., Thompson, P. M., Seifried, B. A., Sulman, E. P., Jensen, S. J., Guo, C., Maris, J. M., Hogarty, M. D., Allen, C., Biegel, J. A., Matisse, T. C., Gregory, S. G., Reynolds, C. P., and Brodeur, G. M. (2001) *Med. Pediatr. Oncol.* **36**, 37–41

KIF1B β Is a Haploinsufficient Tumor Suppressor

8. Brodeur, G. M. (2003) *Nat. Rev. Cancer* **3**, 203–216
9. White, P. S., Thompson, P. M., Gotoh, T., Okawa, E. R., Igarashi, J., Kok, M., Winter, C., Gregory, S. G., Hogarty, M. D., Maris, J. M., and Brodeur, G. M. (2005) *Oncogene* **24**, 2684–2694
10. Hogarty, M. D., Liu, X., Guo, C., Thompson, P. M., Weiss, M. J., White, P. S., Sulman, E. P., Brodeur, G. M., and Maris, J. M. (2000) *Med. Pediatr. Oncol.* **6**, 512–515
11. Nakagawara, A., Ohira, M., Kageyama, H., Mihara, M., Furuta, S., Machida, T., Takayasu, H., Islam, A., Nakamura, Y., Takahashi, M., Shishikura, T., Kaneko, Y., Toyoda, A., Hattori, M., Sakaki, Y., Ohki, M., Horii, A., Soeda, E., Inazawa, J., Seki, N., Kuma, H., Nozawa, I., and Sakiyama, S. (2000) *Med. Pediatr. Oncol.* **35**, 516–521
12. Ohira, M., Kageyama, H., Mihara, M., Furuta, S., Machida, T., Shishikura, T., Takayasu, H., Islam, A., Nakamura, Y., Takahashi, M., Tomioka, N., Sakiyama, S., Kaneko, Y., Toyoda, A., Hattori, M., Sakaki, Y., Ohki, M., Horii, A., Soeda, E., Inazawa, J., Seki, N., Kuma, H., Nozawa, I., and Nakagawara, A. (2000) *Oncogene* **19**, 4302–4307
13. Bauer, A., Savelleva, L., Claas, A., Praml, C., Berthold, F., and Schwab, M. (2001) *Genes Chromosomes Cancer* **31**, 228–239
14. Caron, H., Spieker, N., Godfried, M., Veenstra, M., van Sluis, P., de Kraker, J., Voûte, P., and Versteeg, R. (2001) *Genes Chromosomes Cancer* **30**, 168–174
15. Chen, Y. Z., Soeda, E., Yang, H. W., Takita, J., Chai, L., Horii, A., Inazawa, J., Ohki, M., and Hayashi, Y. (2001) *Genes Chromosomes Cancer* **31**, 326–332
16. Ejeskar, K., Sjoberg, R. M., Abel, F., Kogner, P., Ambros, P. F., and Martinsson, T. (2001) *Med. Pediatr. Oncol.* **36**, 61–66
17. Mosse, Y. P., Greshock, J., Margolin, A., Naylor, T., Cole, K., Khazi, D., Hii, G., Winter, C., Shahzad, S., Asziz, M. U., Biegel, J. A., Weber, B. L., and Maris, J. M. (2005) *Genes Chromosomes Cancer* **43**, 390–403
18. Schwab, M., Praml, C., and Amler, L. C. (1996) *Genes Chromosomes Cancer* **16**, 211–229
19. Schwab, M., Westermann, F., Hero, B., and Berthold, F. (2003) *Lancet* **4**, 472–480
20. Bader, S. A., Fasching, C., Brodeur, G. M., and Stanbridge, E. J. (1991) *Cell Growth & Differ.* **5**, 245–255
21. Sherr, C. J. (2004) *Cell* **116**, 235–246
22. Cook, W. D., and McCaw, B. J. (2000) *Oncogene* **19**, 3434–3438
23. Fodde, R., and Smits, R. (2002) *Science* **298**, 761–763
24. Nagai, M., Ichimiya, S., Ozaki, T., Seki, N., Mihara, M., Furuta, S., Ohira, M., Tomioka, N., Nomura, N., Sakiyama, S., Kubo, O., Takakura, K., Hori, T., and Nakagawara, A. (2000) *Int. J. Oncol.* **16**, 907–916
25. Lawrence, C. J., Dawe, R. K., Christie, K. R., Cleveland, D. W., Dawson, S. C., Endow, S. A., Goldstein, L. S., Goodson, H. V., Hirokawa, N., Howard, J., Malmberg, R. L., McIntosh, J. R., Miki, H., Mitchison, T. J., Okada, Y., Reddy, A. S., Saxton, W. M., Schliwa, M., Scholey, J. M., Vale, R. D., Walczak, C. E., and Wordeman, L. (2004) *J. Cell Biol.* **167**, 19–22
26. Hirokawa, N. (1998) *Science* **279**, 519–526
27. Goldstein, L. S., and Philp, A. V. (1999) *Annu. Rev. Cell Dev. Biol.* **15**, 141–183
28. Nangaku, M., Sato-Yoshitake, R., Okada, Y., Noda, Y., Takemura, R., Yamazaki, H., and Hirokawa, N. (1994) *Cell* **79**, 1209–1220
29. Zhao, C., Takita, J., Tanaka, Y., Setou, M., Nakagawa, T., Takeda, S., Yang, H. W., Terada, S., Nakata, T., Takei, Y., Saito, M., Tsuji, S., Hayashi, Y., and Hirokawa, N. (2001) *Cell* **105**, 587–597
30. Garkavtsev, I., Kazarov, A., Gudkov, A., and Riabowol, K. (1996) *Nat. Genet.* **14**, 415–420
31. Mizuguchi, H., and Kay, M. A. (1998) *Hum. Gene Ther.* **9**, 2577–2583
32. Herman, J. G., Graff, J. R., Myohansen, S., Nelkin, B. D., and Baylin, S. B. (1996) *Proc. Natl. Acad. Sci. U. S. A.* **93**, 9821–9826
33. Tomioka, N., Oba, S., Ohira, M., Misra, A., Fridlyand, J., Ishii, S., Nakamura, Y., Isogai, E., Hirata, T., Yoshida, Y., Todo, S., Kaneko, Y., Albertson, D. G., Pinkel, D., Feuerstein, B. G., and Nakagawara, A. (2008) *Oncogene* **27**, 441–449
34. Gong, T. W., Winnicki, R. S., Kohrman, D. C., and Lomax, M. I. (1999) *Gene (Amst.)* **239**, 117–127
35. Fero, M. L., Randel, E., Gurley, K. E., Roberts, J. M., and Kemp, C. J. (1998) *Nature* **396**, 177–180
36. Blain, S. W., Scher, H. I., Cordon-Cardo, C., and Koff, A. (2003) *Cancer Cell* **3**, 111–115
37. Moll, U. M., LaQuaglia, M., Benard, J., and Riou, G. (1995) *Proc. Natl. Acad. Sci. U. S. A.* **92**, 4407–4411
38. Ichimiya, S., Nimura, Y., Kageyama, H., Takada, N., Sunahara, M., Shishikura, T., Nakamura, Y., Sakiyama, S., Seki, N., Ohira, M., Kaneko, Y., McKeon, F., Caput, D., and Nakagawara, A. (2001) *Med. Pediatr. Oncol.* **36**, 42–44
39. Bagchi, A., Papazoglu, C., Wu, Y., Capurso, D., Brodt, M., Francis, D., Bredel, M., Vogel, H., and Mills, A. A. (2007) *Cell* **128**, 459–475
40. Sells, S. F., Han, S. S., Muthukumar, S., Maddiwar, N., Johnstone, R., Boghaert, E., Gillis, D., Liu, G., Nair, P., Monnig, S., Collini, P., Mattson, M. P., Sukhatme, V. P., Zimmer, S. G., Wood, D. P., Jr., McRoberts, J. W., Shi, Y., and Rangnekar, V. M. (1997) *Mol. Cell Biol.* **17**, 3823–3832
41. Dutta, K., Engler, F. A., Cotton, L., Alexandrov, A., Bedi, G. S., Colquhoun, J., and Pascal, S. M. (2003) *Protein Sci.* **12**, 257–265
42. Joshi, B., Ko, D., Ordonez-Ercan, D., and Chellappan, D. (2003) *Biochem. Biophys. Res. Commun.* **312**, 459–466
43. Bharadwaj, R., and Yu, H. (2004) *Oncogene* **23**, 2016–2027
44. Endow, S. A. (1999) *Eur. J. Biochem.* **262**, 12–18
45. Nakagawara, A. (1998) *Med. Pediatr. Oncol.* **31**, 113–115
46. Nakagawara, A., Arima-Nakagawara, M., Scavarda, N. J., Azar, C. G., Cantor, A. B., and Brodeur, G. M. (1993) *N. Engl. J. Med.* **328**, 847–854
47. Midorikawa, R., Takei, Y., and Hirokawa, N. (2006) *Cell* **125**, 371–383

Plasma midkine level is a prognostic factor for human neuroblastoma

Shinya Ikematsu,¹ Akira Nakagawara,² Yohko Nakamura,² Miki Ohira,² Masaki Shinjo,³ Satoshi Kishida⁴ and Kenji Kadomatsu^{4,5}

¹Department of Bioresources Engineering, Okinawa National College of Technology, Okinawa 905-2192; ²Division of Biochemistry, Chiba Cancer Research Center Research Institute, Chiba 260-8717; ³Department of Public Health and Epidemiology, Okinawa Prefectural College of Nursing, Okinawa 902-0076; ⁴Department of Biochemistry, Nagoya University Graduate School of Medicine, Nagoya 466-8550, Japan

(Received December 23, 2007/Revised June 3, 2008/Accepted June 27, 2008/Online publication October 21, 2008)

Neuroblastoma is the third-most-common solid tumor of childhood. To date, no reliable blood marker for neuroblastoma has been established. The growth factor midkine is highly expressed in human carcinomas and its knockdown leads to tumor growth suppression in animal models. The present study evaluated the plasma midkine level in human neuroblastoma patients. Plasma samples were obtained from patients found through mass screening, as well as from sporadic neuroblastoma patients. The total number of cases examined was 756. Among them, prognostic information was available for 175 sporadic cases and 287 mass-screening cases. Midkine levels were significantly higher in neuroblastoma patients, including both mass-screening cases and sporadic cases, than in non-tumor controls ($P < 0.0001$). The midkine level was significantly correlated with the statuses of *MYCN* amplification, *TRKA* expression, ploidy, stage and age ($P < 0.0001$, < 0.0001 , $= 0.004$, < 0.0001 and < 0.0001 , respectively), which are known prognostic factors for neuroblastoma. There was a striking correlation between high plasma midkine level and poor prognosis ($P < 0.0001$). Within sporadic cases, the midkine level was also strikingly higher than in non-tumor controls ($P < 0.0001$), and correlated with the statuses of *MYCN* amplification and stage ($P = 0.0005$ and $= 0.003$, respectively). There was a significant correlation between high plasma midkine level and poor prognosis ($P = 0.04$). Taken together, the present data indicate that plasma midkine level is a prognostic factor for human neuroblastoma. (*Cancer Sci* 2008; 99: 2070–2074)

Neuroblastoma (NBL) is the third-most-common malignant tumor of childhood, accounting for 15% of cancer-related death.⁽¹⁾ In spite of an enormous amount of research devoted to curing this disease, its prognosis remains poor. NBL has several established prognostic factors, i.e. *MYCN* amplification, *TRKA* expression level, ploidy, stage and age.^(1,2) Cases with tumors with an amplified *MYCN* gene, low *TRKA* expression or diploidy show poor prognosis. Cases at stage 3 or 4, or at ages older than 18 months also show poor prognosis. Since molecular fingerprints within tumor tissues, such as *MYCN* amplification, *TRKA* expression level and ploidy, require a tumor biopsy or its removal, a blood marker for NBL has long been awaited.^(1,2) A blood marker would not only be useful for the initial diagnosis but would also be beneficial for the sequential monitoring of the tumor status.

The growth factor midkine (MK) was originally found in embryonal carcinoma cells, and has been implicated in cancer development.^(3–5) MK is highly and frequently expressed in human carcinomas, including Wilms' tumor, tumors of the digestive tract, brain tumors, urinary bladder tumors and breast tumors, whereas its expression is scarcely detected in normal adult tissues.^(6–10) Strong MK expression is also detected in pre-cancerous stages of human colorectal cancer and human prostate cancer.^(11,12) Knockdown of MK expression leads to suppression

of xenografted tumors of mouse colorectal cancer cells and human prostate cancer cells.^(13,14)

We previously reported that the plasma MK level was correlated with the values of established prognostic factors through a study of 220 cases, including 82 non-mass-screening (sporadic) cases and 122 mass-screening cases.⁽¹⁵⁾ However, in that study, information on the prognosis of patients was too limited to determine whether the plasma MK level could be a prognostic factor. In the present study, we measured plasma MK levels of 756 NBL cases, which consisted of 286 sporadic cases, 387 mass-screening cases and 83 unknown cases. Among them, prognostic information was available for 175 sporadic cases and 287 mass-screening cases. This enabled us to evaluate the plasma MK level as a prognostic factor.

Mass screening for NBL started in 1985 in Japan, but was discontinued in 2004 because of the lack of apparent beneficial effects on the cure rate of NBL. Mass-screening cases are grouped into the favorable prognosis group, and most of the mass-screening cases are thought to have spontaneously regressed. Therefore, nowadays, sporadic NBL patients are the major subject of therapy. However, information obtained from mass-screening cases has been useful, especially to understand tumor phenotype with favorable prognosis. This is the reason why we enrolled 387 mass-screening patients in this study. Accordingly, we evaluated plasma MK levels in two categories: first, the entire set of NBL cases including mass-screening cases and sporadic cases; and second, the set of sporadic cases.

Here we report that the plasma MK level is a prognostic factor for NBL.

Materials and Methods

Plasma samples. Clinical data of 756 neuroblastoma patients are summarized in Table 1. The same archive samples were used as those without malignant tumors ($n = 17$; eleven were <1-year old and six were >1-year old).⁽¹⁵⁾

Enzyme-linked immunoassay for human MK. An enzyme-linked immunoassay for human MK was performed as described previously.⁽¹⁶⁾ Briefly, human MK was produced using *Pichia pastoris* GS115 by transfection with a human MK expression vector, which was constructed into pHL-D4 (Invitrogen, Carlsbad, CA, USA). This yeast-produced human MK was used to immunize rabbits and chickens to raise antibodies. The rabbit antihuman MK antibody (50 μ L of 5.5 μ g/mL in 50 mM Tris HCl (pH 8.2), 0.15 M NaCl, 0.1% NaN₃) was coated onto the wells of microtiter plates (Polysorp plates, Nunc, Rochester, New York, USA) for 20 h at room temperature. After washing with 0.05% Tween-20 in phosphate-buffered saline (PBS), the wells were

^{*}To whom correspondence should be addressed.
E-mail: kkadoma@med.nagoya-u.ac.jp

Table 1. Plasma samples

| | n |
|-----------------------------|-----|
| No malignant tumors | 17 |
| <1 year | 11 |
| >1 year | 6 |
| Neuroblastomas | 756 |
| Stage 1,2,4S | 372 |
| Stage 3,4 | 330 |
| Unknown | 54 |
| MYCN amplification – | 643 |
| MYCN amplification + | 97 |
| Unknown | 16 |
| High <i>TrkA</i> expression | 425 |
| Low <i>TrkA</i> expression | 159 |
| Unknown | 172 |
| Mass screening | 387 |
| Sporadic | 286 |
| Stage 1,2,4S | 62 |
| Stage 3,4 | 209 |
| Unknown | 15 |
| MYCN amplification – | 207 |
| MYCN amplification + | 73 |
| Unknown | 6 |
| High <i>TrkA</i> expression | 109 |
| Low <i>TrkA</i> expression | 113 |
| Unknown | 64 |
| Hyperdiploidy/pentaploidy | 96 |
| Diploidy/tetraploidy | 136 |
| Unknown | 54 |
| <18 months | 101 |
| >18 months | 183 |
| Unknown | 2 |
| Unknown | 83 |
| Hyperdiploidy/pentaploidy | 379 |
| Diploidy/tetraploidy | 263 |
| Unknown | 114 |
| <18 months | 506 |
| >18 months | 242 |
| Unknown | 8 |

blocked with 300 μ L of 0.1% casein, 0.01% Microcide I (aMRSCO) in PBS for 20 h at 37 C. Plasma samples (10 μ L each) were mixed with 100 μ L of 50 mM Tris HCL (pH 8.4), 0.5 M KCl, 0.1% casein, 0.5% bovine serum albumin (BSA), 0.01% Microcide I and 0.1 μ g/mL peroxidase-labeled chicken antihuman MK antibody. Aliquots of 50 μ L of this mixture were added to wells prepared as described above, and further subjected to chromogenic detection at optical density at 450 nm (OD_{450}) using tetramethylbenzidine as the substrate. This assay system shows linearity from 0 to 5 ng/mL of MK, and there is no cross-reaction with pleiotrophin, a close homolog of MK.⁽⁵⁾

Statistical analysis. The Kruskal–Wallis test was used to evaluate the statistical differences between stages. The Mann–Whitney *U*-test was used to further evaluate the difference between the two groups. The Mann–Whitney *U*-test was used for analysis of the other prognostic factors. Survival time was measured from the date of initial diagnosis to the date of death or last contact. The Kaplan–Meier method was used to compare survival between the groups defined by plasma MK levels, and survival differences were analyzed using the log-rank test. All analyses were carried out using StatView for Windows (ver. 5.0; SAS Institute, Cary, NC, USA). $P < 0.05$ was considered statistically significant.

Results

Plasma MK levels of NBL patients and the relationship of plasma MK to established prognostic factors for NBL. The entire set of 756 NBL cases consisted of 387 cases found through mass screening, 286 sporadic NBL cases and 83 unknown cases (Table 1). Plasma MK level of the NBL cases was 23–1 062 520 pg/mL, whereas that of non-tumor controls was 146–517 pg/mL (Fig. 1a). The values of NBL cases were significantly higher than those of controls ($P < 0.0001$). We set the cut-off value average \pm 4SD of non-tumor controls at 900 pg/mL (Fig. 1a). The group of cases with levels higher than 900 pg/mL was designated high MK, whereas cases with lower than 900 pg/mL were grouped into low MK.

MYCN amplification, *TRKA* expression level, ploidy, stage and age are well-known prognostic factors for NBL.⁽¹⁾ The values of each factor were determined for all 756 NBL cases. As shown in Figure 1(b–f), MK levels were significantly correlated with all the prognostic factors. Thus, MK levels were significantly higher in MYCN-amplified cases ($P < 0.0001$, versus MYCN-nonamplified), in cases with low *TRKA* expression ($P < 0.0001$, versus high *TRKA* expression), in diploidy cases ($P = 0.004$), in cases at stage 3 and 4 ($P < 0.0001$, versus stage 1, 2, and 4S) and in cases older than 18 months ($P < 0.0001$, versus younger than 18 months). These groups in which MK levels were high, i.e. MYCN-amplified, low *TRKA* expression, diploidy, stage 3 and 4 and older than 18 months, are known to have a poor prognosis. The data indicate close correlations between MK levels and known prognosis factors and are consistent with our previous report.⁽¹⁵⁾

Figure 2(a) shows Kaplan–Meier survival curves based on plasma MK levels for all NBL cases. A high MK level was closely associated with poor prognosis of NBL patients ($P < 0.0001$), indicating that the MK level alone can be a prognostic factor for NBL patients. It was interesting that a high MK level was associated with poor prognosis within the unfavorable NBL group based on ploidy, i.e. diploidy ($P = 0.02$) (Fig. 2b). This was also the case within favorable NBL groups, that is, groups with MYCN non-amplification, age <18 months or high *TRKA* expression ($P = 0.02$, 0.001 or 0.02, respectively), although the survival differences between high MK and low MK were very small (data not shown).

Analysis for sporadic NBL cases. We examined 286 sporadic NBL cases, among which prognostic information was available for only 175. Plasma MK level was significantly higher in sporadic NBL cases than in non-tumor controls ($P < 0.0001$) (Fig. 3a). It was closely related to the values of two prognostic factors, i.e. MYCN amplification and stage ($P = 0.0005$ and 0.003, respectively) (Fig. 3b,c), but not to those of age, *TRKA* expression level and ploidy (data not shown).

Kaplan–Meier analysis revealed that a high MK level was correlated with poor prognosis in the sporadic NBL patients ($P = 0.04$) (Fig. 4a). The Kaplan–Meier data on MK was further compared with those on known prognostic factors. Survival based on ploidy exhibited a significant difference ($P = 0.025$) (Fig. 4b). MYCN amplification, *TRKA* expression level and stage also showed significant differences ($P = 0.003$, 0.01 and 0.008, respectively), whereas age could not be a prognostic factor for the sporadic NBL cases examined (data not shown). The Cox hazard ratio was 1.71 for MK level, 2.27 for ploidy, 2.70 for MYCN amplification, 2.38 for *TRKA* expression and 1.84 for stage.

Discussion

In the present study, we first evaluated the plasma MK level using the entire set of NBL cases including both the mass screening and sporadic cases. As predicted from our previous data,⁽¹⁵⁾ we found that MK level is correlated with established prognostic factors (MYCN, *TRKA*, ploidy, stage and age). Since

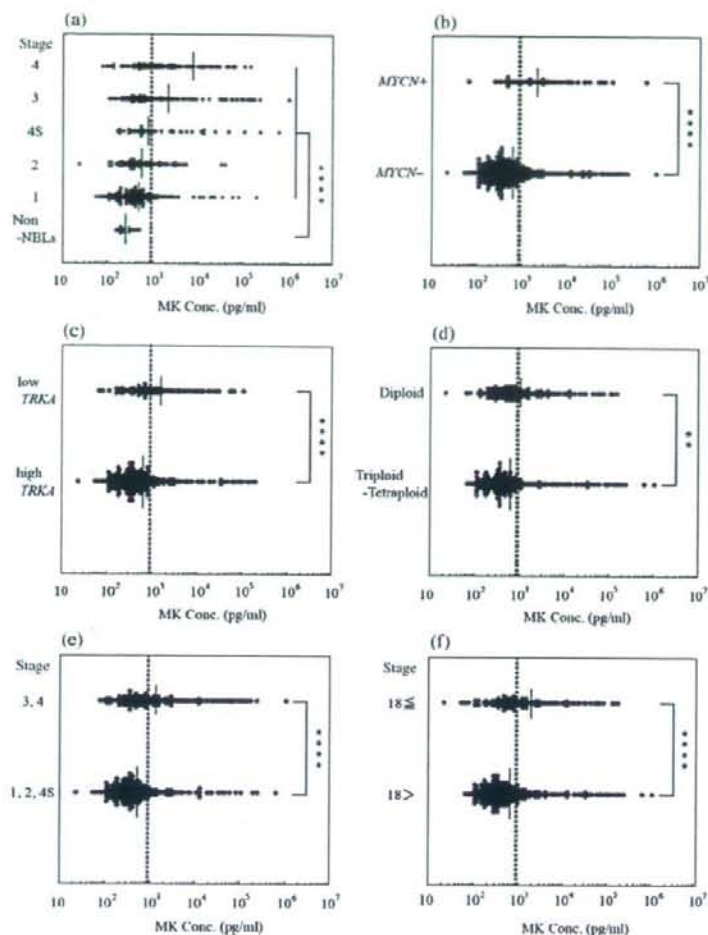


Fig. 1. Plasma midkine (MK) levels of the entire set of neuroblastoma (NBL) cases and the relationship of MK level to established prognostic factors for NBL. Blood MK levels are presented with dots. Each dot represents a NBL patient or a non-NBL control as indicated. (a) MK level distribution of the NBL patients through stages. Non-NBL, non-NBL controls. **** $P < 0.0001$. (b) NBL cases divided into *MYCN* amplification (*MYCN*+) and nonamplification (*MYCN*-). **** $P < 0.0001$. (c) NBL cases divided into low *TRKA* expression (low *TRKA*) and high *TRKA* expression (high *TRKA*). **** $P < 0.0001$. (d) NBL cases divided into diploid and triploid/pentaploid. ** $P = 0.004$. (e) NBL cases divided into stage 3 or 4 (Stage 3, 4) and stage 1, 2 or 4S (Stage 1, 2, 4S). **** $P < 0.0001$. (f) NBL cases divided into age >18 months and <18 months. **** $P < 0.0001$.

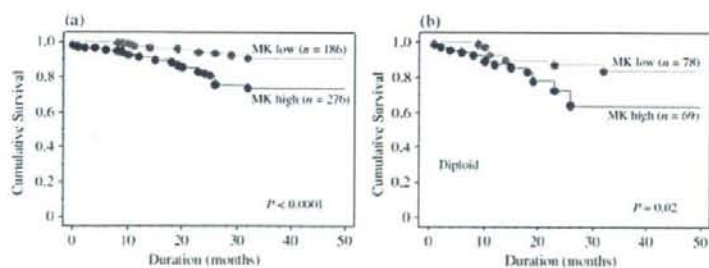


Fig. 2. Kaplan-Meier curves for neuroblastoma (NBL) cases. 'MK low' was defined as a blood midkine (MK) level less than 900 pg/mL, whereas 'MK high' was more than 900 pg/mL. Cumulative survival rates of MK low and high groups were estimated for the entire set of NBL cases (a) and cases with diploidy (b).

mass screening has been discontinued, sporadic NBL are the major subject of therapy. We therefore further evaluated the MK level of only the sporadic cases. Our study revealed that, within sporadic cases, blood MK level alone could be a predictor of prognosis. MK level was also significantly correlated with *MYCN* amplification and stages.

However, blood MK level could not predict prognosis of patients in the intermediate risk group (*MYCN* non-amplification and stage 3 or 4) (data not shown). It could not predict the prognosis

of patients within the high-risk group or low-risk group either (data not shown). This indicates that a single molecule may not be satisfactory for predicting the prognosis or judging the precise status of NBL for the decision of therapy, since, like other carcinomas, a complex of molecules is thought to contribute to carcinogenesis and development of NBL.^(17,18) There are several blood markers predicting clinical outcome of neuroblastoma patients; i.e. serum lactate dehydrogenase, ferritin, neuron-specific enolase, disialoganglioside GD2 and NM23H1.⁽¹⁹⁻²³⁾ Therefore,

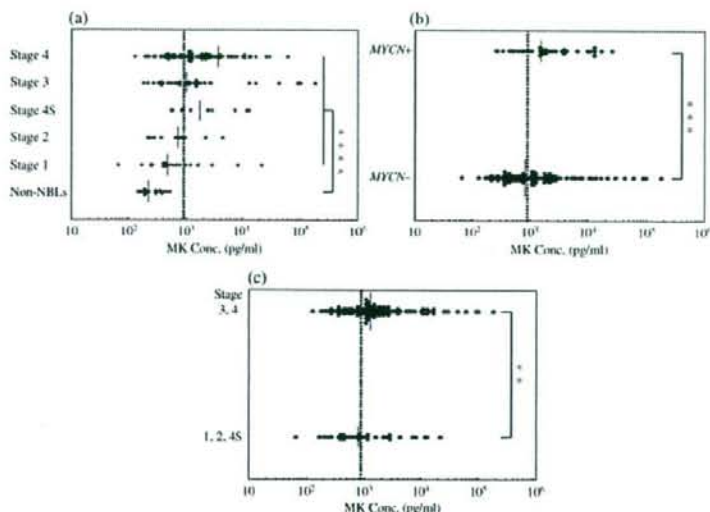


Fig. 3. Analysis for sporadic neuroblastoma (NBL) cases. Blood midkine (MK) levels of sporadic NBL cases are shown. (a) MK level distribution of the sporadic NBL patients through stages. Non-NBLs, non-NBL controls. **** $P < 0.0001$. (b) Sporadic NBL cases divided into *MYCN* amplification (*MYCN*+) and non-amplification (*MYCN*-). *** $P = 0.0005$. (c) Sporadic NBL cases divided into stage 3 or 4 (Stage 3, 4) and stage 1, 2 or 4S (Stage 1, 2, 4S). ** $P = 0.003$.

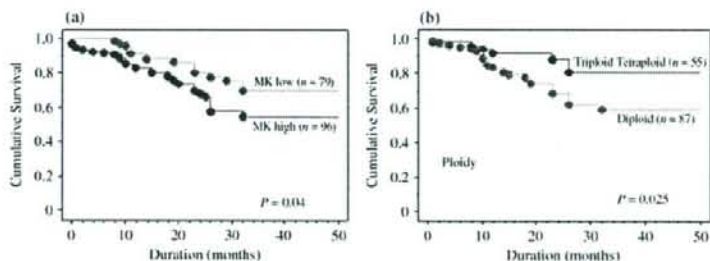


Fig. 4. Kaplan-Meier curves for sporadic neuroblastoma (NBL) cases. Cumulative survival rates of sporadic NBL cases were compared based on the following criteria. (a) Midkine (MK) low or high. (b) Diploid or triploid/pentaploid.

it is reasonable to expect that a combination of the plasma levels of MK and other blood biomarkers will facilitate accurate prognosis and accurate evaluation of tumor status. In addition, many efforts are being made to identify molecular changes associated with NBL with unfavorable prognosis.^(17,18) Such studies will provide other biomarkers for NBL.

It is interesting that MK levels of stage 4s were lower in the present study than those in the previous study. Twelve cases were only available for stage 4s in the previous study. In the present study, 39 cases of stage 4s were available for the analysis of the entire set of NBL (Fig. 1a) and 15 cases for the sporadic NBL (Fig. 3a). Therefore, it is conceivable that midkine level deduced in the present study is more reliable because of the increased number of cases analyzed.

This is the first report indicating the plasma MK level as a prognosis factor for a human carcinoma. MK is frequently and highly expressed in malignant tumors regardless of the tissue type,⁽⁵⁾ similar to mutations in the p53 gene. An elevated serum MK level is also detected in more than 80% of human adult carcinomas.⁽¹⁶⁾ Although the MK level has not been evaluated as

a prognosis factor for human carcinomas except for NBL, further assessment of the MK level will be useful in potentially establishing it as a new biomarker for other carcinomas.

Tumor growth is suppressed by the knockdown of MK expression.^(13,14) MK is barely detectable in normal adult tissues. Furthermore, the present study has established that high blood MK level is closely related to poor prognosis, at least in NBL. Therefore, our data also support the idea that MK is a candidate molecular target for cancer therapy. Indeed, MK-deficient mice carrying a *MYCN* transgene show delayed development of NBL as compared with wild-type mice (Kishida and Kadomatsu, unpublished data). A therapy targeting MK for NBL is currently being studied in our laboratory.

Acknowledgments

We thank Tohru Doi for a critical reading of this manuscript. This work was supported by Grants-in-Aid from the Ministry of Education, Science, Sports, Culture (15COE01-09, 18790218) and a Grant-in-Aid from the Ministry of Health (CAN16K16).

References

- Brodeur GM. Neuroblastoma: biological insights into a clinical enigma. *Nat Rev Cancer* 2003; 3: 203-16.
- Henry MC, Tashjian DB, Breuer CK. Neuroblastoma update. *Curr Opin Oncol* 2005; 17: 19-23.
- Kadomatsu K, Tomomura M, Muramatsu T. cDNA cloning and sequencing of a new gene intensely expressed in early differentiation stages of

- embryonal carcinoma cells and in mid-gestation period of mouse embryogenesis. *Biochem Biophys Res Commun* 1988; 151: 1312-18.
- Tomomura M, Kadomatsu K, Nakamoto M *et al*. A retinoic acid responsive gene, MK, produces a secreted protein with heparin binding activity. *Biochem Biophys Res Commun* 1990; 171: 603-9.
- Kadomatsu K, Muramatsu T. Midkine and pleiotrophin in neural development and cancer. *Cancer Lett* 2004; 204: 127-43.
- Tsutsui J, Kadomatsu K, Matsubara S *et al*. A new family of heparin-binding